Review

Antimicrobial Properties of the Ag, Cu Nanoparticle System

Xinzhen Fan [1], L'Hocine Yahia [1] and Edward Sacher [2,*,†]

1   Laboratoire d'Innovation et d'Analyse de Bioperformance, Département de Génie Mécanique, Polytechnique Montréal, CP 6079, Succursale C-V, Montréal, QC H3C 3A7, Canada; Xinzhen.fan@polymtl.ca (X.F.); lhocine.yahia@polymt.ca (L.Y.)

2   Département de Génie Physique, Polytechnique Montréal, CP 6079, Succursale C-V, Montréal, QC H3C 3A7, Canada

*   Correspondence: edward.sacher@polymtl.ca

†   Submitting author.

Simple Summary: The antimicrobial properties of Ag and Cu nanoparticles, their mixtures and their alloys, are reviewed.

Abstract: Microbes, including bacteria and fungi, easily form stable biofilms on many surfaces. Such biofilms have high resistance to antibiotics, and cause nosocomial and postoperative infections. The antimicrobial and antiviral behaviors of Ag and Cu nanoparticles (NPs) are well known, and possible mechanisms for their actions, such as released ions, reactive oxygen species (ROS), contact killing, the immunostimulatory effect, and others have been proposed. Ag and Cu NPs, and their derivative NPs, have different antimicrobial capacities and cytotoxicities. Factors, such as size, shape and surface treatment, influence their antimicrobial activities. The biomedical application of antimicrobial Ag and Cu NPs involves coating onto substrates, including textiles, polymers, ceramics, and metals. Because Ag and Cu are immiscible, synthetic AgCu nanoalloys have different microstructures, which impact their antimicrobial effects. When mixed, the combination of Ag and Cu NPs act synergistically, offering substantially enhanced antimicrobial behavior. However, when alloyed in Ag–Cu NPs, the antimicrobial behavior is even more enhanced. The reason for this enhancement is unclear. Here, we discuss these results and the possible behavior mechanisms that underlie them.

Keywords: antibacterial; biofilm; metal nanoparticles

1. Introduction

As the antibiotic resistance of microbes to drugs grows, nanotechnology provides us an opportunity to resolve this problem [1,2]. Metal NPs, referred to as nanobiotics, have been proposed as novel antimicrobial agents. They have the potential to reduce or eliminate the continuous emergence of bacterial resistance [3]. The metals used for these NPs are almost exclusively heavy metals, such as Ag and Cu.

Ag has been utilized as an antimicrobial agent for several millennia, since Hippocrates prescribed the use of Ag to treat ulcers [4,5]. As nanotechnology has developed [6], Ag NPs have become widely used in antimicrobial applications, especially in combatting antibiotic-resistant bacteria and nosocomial infections [5]. As for Cu, its antiseptic potential was recorded four thousand years ago [7]. Indeed, the first report of Cu as an antimicrobial agent predates that of Ag. Despite this, antimicrobial studies of Ag are more common than those of Cu. What is noteworthy is that, compared to the large number of antimicrobial studies of Ag or Cu, the number of the publications involved in the combination of antimicrobial Ag and Cu nanomaterials is only approximately 300, so far (Figure 1).

Despite this, their exact antimicrobial mechanisms are still elusive. Currently proposed theories all have limitation, and cannot explain the antimicrobial activities in all situations. Recently, AgCu nanoalloys were reported to have antimicrobial properties far greater than either Ag or Cu NPs [8,9]. As it is the NP surface that participates in all the

proposed mechanisms, it is our position that the physicochemical surface characterization of NPs, particularly their surfaces, will determine the actual reason(s) behind antimicrobial behavior. It is our purpose to discuss and summarize the antimicrobial activities of Ag and Cu NPs, their combinations and alloys.
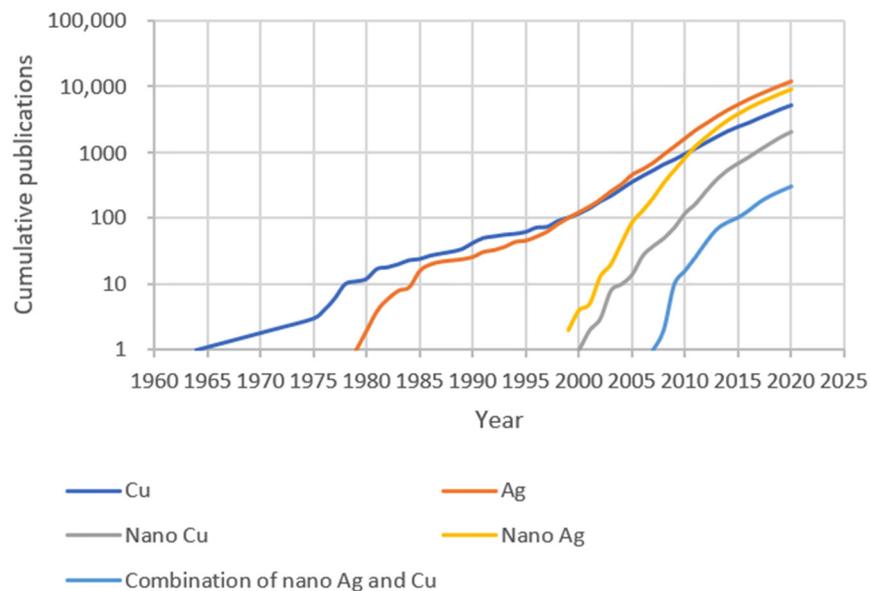
Figure 1. Cumulative numbers of publications on antimicrobial Cu and Ag, as of 1 December 2020. The bibliometric data were searched in the Polytechnique Montréal library Compendex database, as indicated in the Appendix A.

2. Biofilm Contamination

2.1. Bacteria and Fungi

The majority of bacteria can be classified into two types: Gram-positive and Gram-negative. The main difference between such bacteria is their cell structures: Gram-positive bacteria have a thick layer of peptidoglycan in the cell walls, while the peptidoglycan layer of Gram-negative bacteria is thinner, and covered with another lipid membrane. Mostly, *Staphylococcus aureus* is used to represent Gram-positive bacteria, and *Escherichia coli*, Gram-negative bacteria, in antibacterial experiments. Some researchers have found Gram-positive bacteria to be more sensitive to NPs, because they consider the cell wall structure of Gram-negative bacteria to be more complex [10,11]. In contrast, other researchers believe that Gram-negative bacteria are more susceptible to antibacterial Ag NPs, as it is easier for Ag ions to penetrate the thinner cell walls of Gram-negative bacteria [12,13].

Contamination by fungi has also become a significant healthcare concern. Due to the presence of fungal eukaryotic cells, infections caused by fungi are more difficult to diagnose and treat than those caused by bacteria [14]. The most common fungus, *Candida albicans* [15], can survive, proliferate and spread for several weeks, on either dry or wet surfaces, and may cause bloodstream infections that have a high mortality rate. It has been reported that Ag NPs can inhibit the growth of fungal strains, and further damage fungus cells [16–18]. By contrast, Cu NPs exhibit favorable antifungal efficiency mainly in the field of fungus-induced plant diseases, rather than of human diseases [19–21]. However, Ag, Cu, and AgCu nanoalloy NPs cannot inhibit and kill *Candida albicans* as efficiently as they can *E. coli* and *S. aureus* [22].

2.2. Biofilm and Planktonic Microbes

Biofilms are clusters of microbes (bacteria, fungi) with an extracellular matrix made up of polymeric substances, such as polysaccharides, proteins, lipids, nucleic acids, and humic substances, which attach to inert or living surfaces [23–25]. Extracellular polymeric

substances may play the role of a protective shelter, or a diffusion barrier. Therefore, biofilms are stable enough to resist physical forces, pH changes, oxygen radicals, as well as antibiotics and phagocytosis [26,27]. Although, in some cases, the strains are comprised of different species of microbes, the biofilms produced are still stable, or often even more stable [28]. In hospitals or clinics, biofilm formation on the surfaces of medical instruments may cause nosocomial infections [29]. Similarly, such formation on the surfaces of implants lead to orthopedic implant infections [30].

Planktonic microbes are free-living microbes, which may float or swim in a fluid medium. Compared to biofilms, it is generally believed that planktonic microbes are more susceptible to antimicrobial agents such as NPs [31,32], because NPs must aggregate and interact with the extracellular polymetric substances produced in biofilms, thereby decreasing their toxicity to microbial cells [33]. Thus, the antibiotic resistance of biofilms is much greater than that of planktonic bacteria [34].

2.3. Biofilm Formation and Prevention

Nosocomial infections are a significant source of human morbidity and mortality, which affects millions of patients annually [35]. It is generally believed that planktonic bacteria attaching to the surfaces of medical devices, or public items in hospitals, may proliferate to form the initial thin biofilm. When growing to mature biofilms, planktonic bacterial cells may disperse, attacking new surfaces, and starting new life cycles (Figure 2) [24]. Ultimately, biofilm-caused contamination may spread to some key hospital areas, such as intensive care units (ICUs) [36].
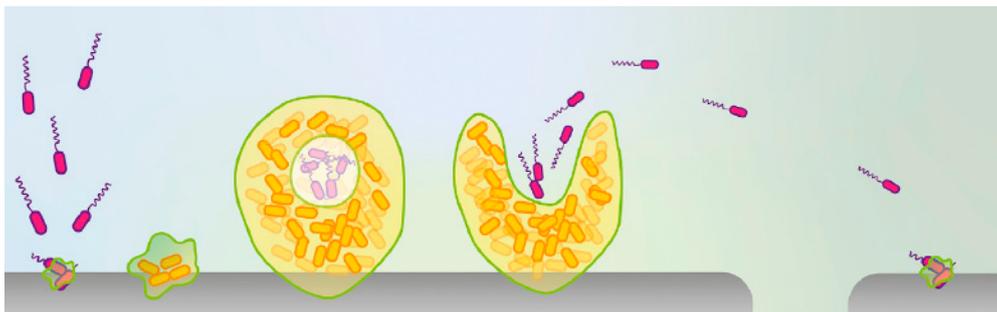

Figure 2. Life cycle of biofilm. Reproduced with permission from Ref [24]. Copyright 2019, Elsevier.

Recently, another model was proposed to explain biofilm formation (Figure 3). This model proposes that multicellular aggregates can form biofilms more easily than single cells [37]. This model is more likely to correspond to biofilm formation in natural environments, in which the microbes form and disperse biofilms in the pattern of multicellular aggregates, instead of single cells [37].

Cells descending from single cell attachment ● Cells descending from pre-formed aggregate attachment ▯ Biofilm matrix
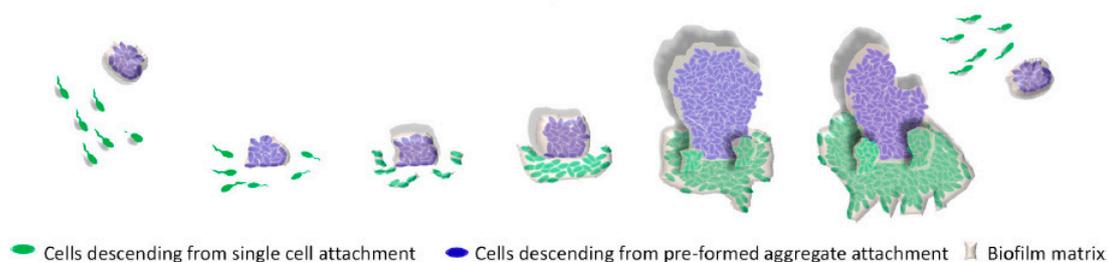
Figure 3. New model of biofilm formation. Reproduced with permission from Reference [37]. Copyright 2016, American Society for Microbiology.

Implants (e.g., mesh [38], dental [39], breast [40]), and other prostheses [30], also risk biofilm contamination. A mechanism of bacterial attachment on implant surfaces was

proposed, involving a two-phase attachment process: physical factors, including Brownian motion, van der Waals attraction, and surface electrostatic forces, contribute to the initial phase of the interaction, followed by molecular reactions between the implant surface and the bacterial surface polymeric structure, which can result in stronger interfacial adhesion [41–44].

Patients, following surgery, may have to face the serious consequences of nosocomial and postoperative infections, and their associated high health costs [45]. Microbes, accumulated on implant surfaces, can trigger tissue inflammation, which results in osteolysis, and even bone loss [46]. Because biofilm-mediated infections on implants occur inside human bodies, they are difficult to detect and treat, so that the best method to resolve this problem is to prevent biofilm formation in the first place. Designing antimicrobial implant surfaces, such as by coating them with NPs, is currently being studied [47,48]. Implant surfaces, functionalized in this manner, were found to have not only bactericidal properties, but also resistance to bacteria adhesion [49]. There are various explanations for why nanostructured surfaces are thought to prevent biofilm formation. The sharp edges of nanostructures may destroy microbial membranes, and would also be toxic to human cells [50]. Theoretically, the hydrophilicities of the substrate and different microbial cell surfaces are related to microbial adhesion [46]. Surfaces coated with a high density of NPs can limit the adhesion of Gram-positive bacteria, because of the rigid peptidoglycan membrane, which is difficult to flex and adapt to the nanostructured surface [51]. Roughness is also believed to be related to biofilm formation: surfaces with elevated rugosities favor biofilm formation [46]. Apart from surface structure-based antimicrobial activity, NPs also have intrinsic antimicrobial mechanisms.

3. Antimicrobial Mechanisms

Although the precise antimicrobial mechanisms of NPs are still not known, several hypotheses have been proposed, such as the release of metal ions [12,52], antimicrobial behavior mediated by reactive oxygen species [53], direct interaction between NPs and microbes (i.e., contact killing) [54], a combined (comprehensive) mechanism [55], and immunostimulatory effects [56]. The antiviral potential of NPs is discussed in this section, as well.

3.1. Released Ions

Many research groups [57–60] believe that the main antimicrobial mechanism is the release of ions from NPs. That is, Ag NPs only function as vehicles to transport and deliver Ag ions for interaction with bacteria, in which the Ag ions exerted the main antimicrobial effect (Figure 4) [61]. In order to clarify the antimicrobial mechanism, the antimicrobial property of Ag nitrate solution was evaluated against *E. coli* [62], which found that Ag ions interact with membrane proteins to change the membrane permeability. The mechanism of protein deactivation is probably dependent on the reaction of Ag ions with cysteine residues [63]. After the released ions enter bacterial cells, DNA and RNA, and their transcriptional responses, are affected [57]. In other research, in order to eliminate the influence of the NPs themselves, NPs were confined in a matrix, which only permitted ion generation and release [64]; the results showed good antibacterial properties, which demonstrated the key role of ions in antimicrobial activity.
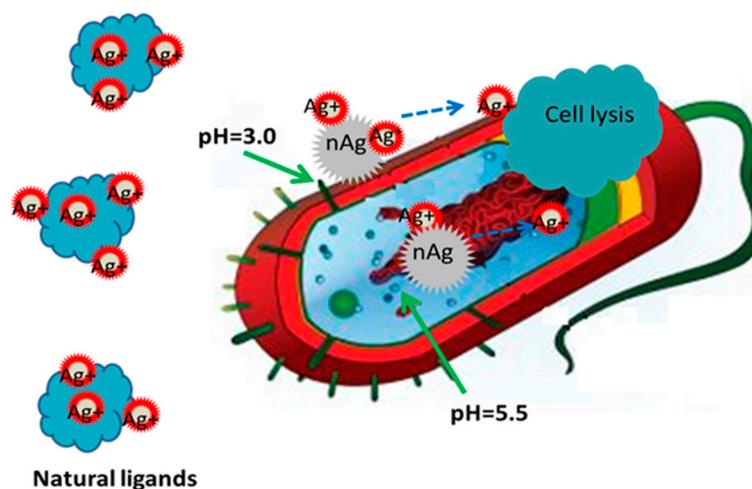
Figure 4. Ag NPs function as vehicles to deliver Ag ions to interact with bacterial cytoplasm and membrane, decreasing the local pH. Reproduced with permission from Reference [61]. Copyright 2012, American Chemical Society.

It was also shown that antimicrobial efficacy is based on the surface charge of Ag NPs, in which positively charged Ag NPs exhibit higher antimicrobial effectiveness than those negatively charged [65]. Generally, the surface charge can be altered through conjugating different capping agents. The cell walls of both Gram-positive [66] and Gram-negative [67] bacteria are negatively charged. Therefore, the greater the positive NP surface charge, the lower the electrostatic barrier. As a result, positively charged Ag NPs interact more readily with bacteria and exhibit greater antibacterial properties [68].

3.2. Reactive Oxygen Species

Reactive oxygen species (ROS) are short-lived, highly reactive molecules containing oxygen. Typically, they consist of unstable oxygen free radicals, including hydroxyl radical ($\bullet OH$), peroxide ($O_2 \bullet^{-2}$) and superoxide ($O_2 \bullet^{-}$) anions, and non-radicals, such as hydrogen peroxide (H_2O_2) and hydroxyl ions (OH^{-}) [69,70]. Normally, ROS are generated and consumed by cells under dynamic balance. If the generation of ROS surpasses the antioxidant capacity of microbial cells, oxidative stress may be induced [71]. Such oxidative stress is liable to damage intracellular biomacromolecules, such as proteins, lipids, RNA and DNA [72–76].

Different ROS exhibit different antimicrobial capacities. The commonly discussed ROS in antimicrobial activity are OH^{-}, H_2O_2, and $O_2 \bullet^{-}$. Some negative ROS, such as OH^{-}, are prone to interact with positively charged microbial cell membranes, although H_2O_2 is more efficient in penetrating cell membranes [77,78]. Interestingly, one report indicates that ROS can maintain cell membranes intact and simultaneously destroy intracellular biomolecules [79].

Ions released from NPs under humid circumstances can induce ROS generation. Electrons released from Ag NPs have been found to lead to bursts of ROS in both extracellular and intracellular environments (Figure 5) [80]. The oxidative stress induced by excess ROS can destroy biomolecules; once a ROS scavenger, such as acetylcysteine, is added, the antimicrobial activity of Ag NPs is noticeably restrained, confirming that bacteria can be killed by NP-induced excess ROS production.
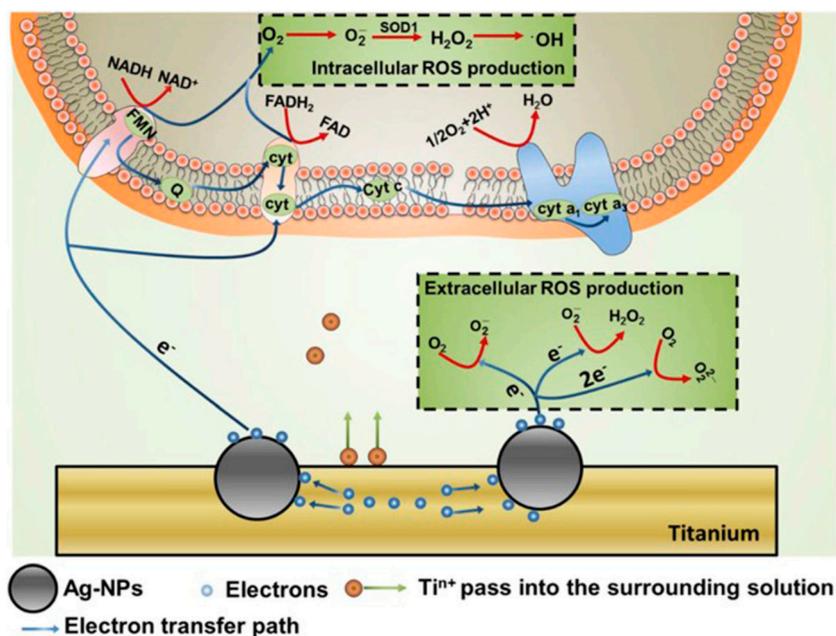
Figure 5. Production of ROS outside and inside bacterial cells. Reproduced with permission from Reference [80]. Copyright 2017, Elsevier.

3.3. Contact Killing

Some research has demonstrated that NPs possess antimicrobial properties under dry conditions [81,82], indicating that direct contact appears to be a potential antimicrobial mechanism. In a dry environment, no electrochemical reactions occur on the surface of NPs, so ions and electrons are not released to interact with biomolecules, or induce ROS bursts. It is posited that Cu NPs interact with membrane proteins [83], and penetrate into bacterial cells [84], inducing an explosion of ROS in the intracellular environment (Figure 6) [85]. Experiments have shown that the production of ions cannot increase the antibacterial effect of Cu NPs [81].
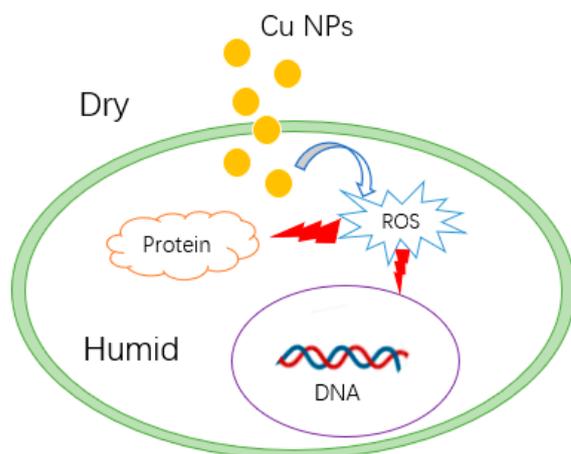
Figure 6. Possible contact killing mechanism of Cu nanoparticles (NPs).

In some studies, Ag NP were found to show good antimicrobial properties under circumstances where no Ag ions could be detected [86]. Additionally, control experiments were carried out to compare the antimicrobial efficiencies of Ag NPs and Ag ions, which indicate that NPs were more effective against *E. coli* than ions [87]. It was reported that the concentration of released ions from different sizes of Ag NPs was essentially identical, while their antibacterial activities were different, implying that contact killing was the

dominate antibacterial factor [88]. Another example, based on a comparison between immobilized and colloidal Ag NPs [89], also implied that contact killing was the predominant antimicrobial mechanism. As well, the formation of porous structures and holes on the *E. coli* cell surface, when attaching to Ag NPs, is evidence of contact killing [90]. However, most studies were not conducted under absolutely dry conditions, which would have eliminated the possible effect of ions and ROS.

3.4. Combined Antimicrobial Mechanism

NP antimicrobial activity does not appear to be dependent on any one individual hypothesis. Rather, the previously cited mechanisms (NPs, released ions, and ROS) should all be considered, with several possibly operating synergistically in the antimicrobial process.

In terms of this hypothesis, all may simultaneously exercise their own separate roles [55,91,92]. As an example, Ag NPs may accumulate on the bacterial cell walls and membranes, and regulate membrane proteins [93], changing the membrane permeability to permit both Ag NP and ion transport into bacteria cells. Ag NPs that have penetrated into cells, continue to release ions, which can attack proteins and DNA. Intracellular ROS are produced by Ag ions, which may also affect proteins and DNA (Figure 7) [55].
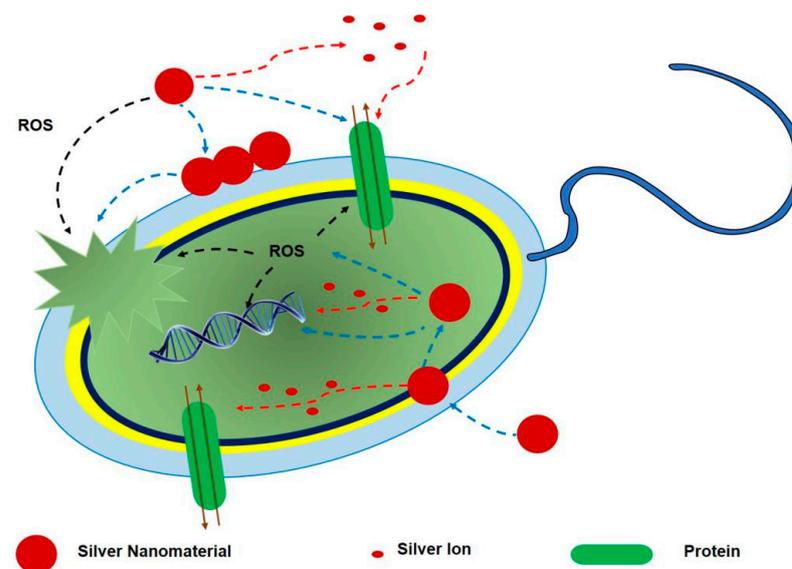
Figure 7. The comprehensive mechanism of antibacterial activity of Ag NPs. Reproduced with permission from Reference [55]. Copyright 2018, John Wiley and Sons.

3.5. Immunostimulatory Effects

In addition to direct killing, NPs can also modulate immune responses, and enhance innate antimicrobial immune defenses [56]. Reactive nitrogen species (RNS), like ROS, are important in the antimicrobial process [94]. Ag and Cu NPs can cause an increase in the concentration of nitric oxide, one kind of RNS, resulting in a synergistic host immune defense against microbes [95,96]. Nitric oxide can also oxidize Cu, present in protective proteins in microbes, to free Cu ions, which boosts toxicity to microbial cells [56].

In addition to RNS, antimicrobial peptides are abundant natural antibiotics, produced by humans, which play a significant antibiotic role in the immune system [97,98]. Both Ag and Cu NPs exhibit synergistic antimicrobial effects with polymyxin B, one type of antimicrobial peptide [56,99].

Adjuvants are often used in vaccine production to improve the immune response [100]. Ag NPs, used as vaccine adjuvants, can dramatically induce the increase of the antigen-specific IgG1/IgG2a ratio, as well as antigen-specific IgE. Local leukocytes, particularly macrophages, are also activated by Ag NPs [101].

Although the immunostimulatory effect of NPs has been proposed as a possible antimicrobial mechanism, the relevant reports are still scarce.

3.6. Antiviral Mechanism

In the context of the COVID-19 pandemic and its ongoing vaccine development, research on effective antiviral agents is urgent. It has been reported that the survival time of the coronavirus on different materials, such as metal, paper, plastic, and glass, varies from a few hours to days [102]. Because of their ability to interact with proteins, DNA and RNA, metal NPs have the potential to destroy viruses.

One possible NP antiviral mechanism was proposed as occurring in three stages (Figure 8): (1) interaction with the viral protein shell, to restrain its attachment to human cells; (2) production of ions and ROS, which destroy the viral protein shell, and DNA or RNA; (3) NP penetration into the cell, followed by interaction with enzymes, to prevent viral replication and subsequent spread [103,104].
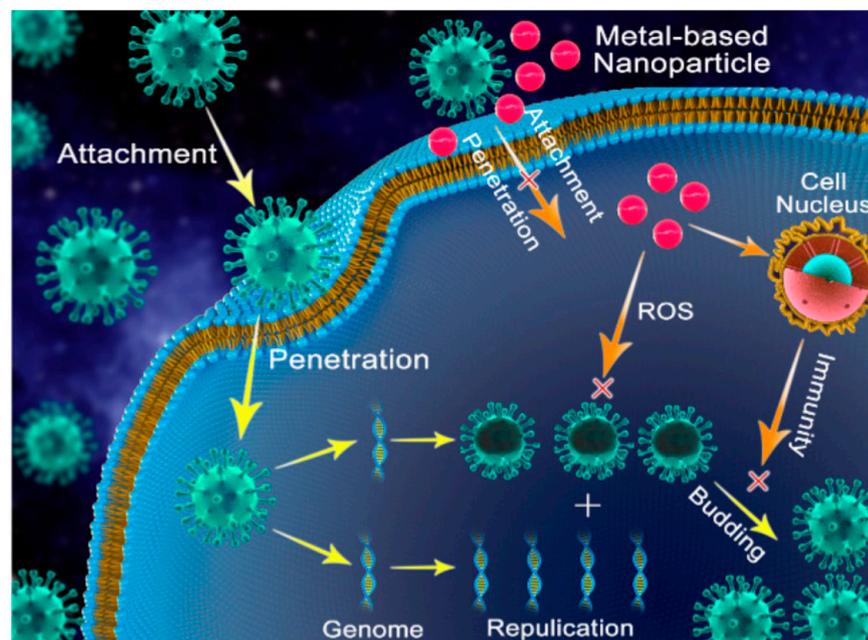
Figure 8. Possible antiviral mechanism of metal NPs. Reproduced with permission from Reference [103]. Copyright 2020, Springer Nature.

Ag NPs have been shown to have a high antiviral capability toward the African swine fever virus, through interacting with its protein shell, and thereby preventing viral penetrating into the animal's cell [105]. One study, involving Ag$_2$S NPs, indicated that the antiviral capacity predominantly influences the stages of viral RNA replication and budding [106]. Both naked Ag NPs and those coated with polysaccharide, poly N-vinyl-2-pyrrolidone, and mercaptoethane sulfonate, exhibit activity toward HIV, TCRV, RSV, HBV, MPV, and HSV viruses [107]. Due to their broad-spectrum antiviral properties, Ag NPs have the potential to be used as antiviral drug.

Cu NPs also display excellent antiviral behavior. Cu was found to inactivate norovirus through inhibiting its RNA replication while its protein shell remained intact, which suggests that ions penetrated into the virus to act against the RNA [108]. CuO NPs, with an average size of 40 nm, exhibited effective inhibition of *Herpes simplex* virus type 1 (HSV-1), although the antiviral effectiveness was not as good as that of the conventional antiviral medicine, acyclovir [109].

4. Ag and Cu NPs

The difference in antimicrobial ability between Ag and Cu NPs was initially thought to depend on the different amounts of ions released [110]. The activity of Cu was found to be greater than that of Ag, and, at the same NP concentration, ions released from Cu NPs were found to be at a higher concentration [111]. However, the antimicrobial ability of Ag NPs was found to be greater than that of Cu NPs, indicating that Ag ions are more efficient in antimicrobial activity than Cu ions [111,112]. Ag NPs also show broader antimicrobial effectiveness to various strains of *E. coli* and *S. aureus*, as well as to fungi [113], which may be due to their stronger interaction with polysaccharides and proteins on cell walls [114]. The existence of an oxide layer on Cu NPs was proposed to be the reason that the antimicrobial capacity of Cu NPs is less than that of Ag NPs [115,116].

4.1. Influence of Size and Shape

Size has a considerable influence on antimicrobial properties. For a given mass, the smaller the NP size, the higher the surface:volume ratio, which increases the antimicrobial capacity, as ions can be more rapidly released [63,79,117]. Ag NPs synthesized from green and black tea leaf extracts have shown superior antimicrobial properties than Cu NPs produced by the same method, because the size of the Ag NPs produced is smaller [118]. However, others have suggested that size does not have much of an influence on the antimicrobial properties, rather that surface charge is the most significant influence factor [65]. Another study showed that larger sized Ag nanoclusters can release higher concentrations of ions, although the antimicrobial effect was not influenced to a great extent [119]. However, size may not be the most significant antimicrobial factor, as another study revealed that larger Ag NPs are more effective than smaller ones [65].

Nanocrystal shapes are produced by controlling growth speeds along different crystallographic directions [120]. Antimicrobial properties are also impacted by different NP shapes. Truncated triangular and spherical Ag NPs are more effective than Ag nanorods [121]. Another study reached a similar conclusion: hexagonal Ag NPs, similar to truncated triangular NPs, show better antimicrobial effects than spherical and triangular shapes [122]. These results may indicate that antimicrobial effects are not related to size, because the weakest triangular NPs have the largest surface areas at a given volume. If the surface area determined antimicrobial properties, smaller sized NPs, with higher surface areas, would have stronger antimicrobial activities. However, this is not what was found. One study indicated that the (1, 1, 1) facet might be able to enhance antimicrobial property because it can generate singlet oxygen (one type of ROS), under photo-irradiation, while other facets do not have this function [120,123]. Anisotropic Ag NPs exhibit higher antimicrobial effects than spherical ones, which is attributed to a greater number of crystal (1, 1, 1) facets.

In addition to size and shape, the existence of corners, edges, defects and deformations on the microstructure may also influence the antimicrobial effect [110].

4.2. Influence of Surface Treatment

Chemical agents or surface treatments may enhance the antimicrobial abilities of NPs. In one study, Cu-loaded silica nanomaterial showed improved antimicrobial efficacy over bare Cu NPs, while Ag-loaded silica did not show better antimicrobial ability, when compared with plain Ag NPs [124]. Surfactants, including SDS, Tween 80, and PVP, can stabilize NPs against aggregation, which can enhance their antimicrobial properties [125]. Cu NPs, coated with starch macromolecules, showed more efficient antimicrobial efficacy than Ag NPs, the starch coating being capable of reducing oxidized Cu [126]; other coatings did not influence their antimicrobial properties. Both Ag and Cu NPs were grafted onto the surfaces of carbon nanotubes; the Ag-grafted carbon nanotubes were found to have greater antimicrobial properties than the Cu-grafted ones, while the pure carbon nanotubes had the poorest antimicrobial performance [127]. In the case of argon plasma surface treatment, the antimicrobial effect of polymer surfaces coated with Cu NPs was greater than those

coated with Ag NPs, perhaps because the surface roughness of the polymers coated with Cu NPs was greater than that of the surfaces coated with Ag NPs, resulting in greater exposure to microbes [60].

To overcome microbial resistance to either NPs or conventional antibiotics, the functionalization of NPs with antibiotics appears to be promising. The synergistic antimicrobial effect of the combination of Ag NPs and antibiotics was found to be much greater than Ag NPs or antibiotics, alone [128,129]. Similar to Ag, Cu NPs, combined with various antibiotics, particularly ampicillin, had increased antimicrobial properties [130]. The enhancement of microbial susceptibility to the combination of NPs and antibiotics may result from the higher permeability of microbial cell walls, modulated by NPs, which can facilitate the entry of antibiotics into cells; another reason may be that the enzymes, which play key roles in the antibiotic resistance, are inactivated by NPs [131].

4.3. Oxide NPs

In general, both Ag oxide and Cu oxide NPs are considered to belong to the set of Ag and Cu NPs, because Ag and Cu NPs oxidize when exposed to atmosphere. Theoretically, Cu NPs are easier to oxidize than Ag [111]. Despite the low number of articles on antimicrobial Ag oxide (i.e., Ag_2O and $Ag^IAg^{III}O_2$) NPs, they appear to show antimicrobial properties [132–134]. It is believed that AgO is the most active against microbes [8]. In contrast to Ag oxides NPs, there is a large number of reports on Cu oxide NPs, including both Cu_2O and CuO. For Cu NPs deposited onto the surface of TiO_2, they were shown to be covered with a thin mixed CuO, Cu_2O layer [29]. The mechanism of contact killing, described earlier, deals mostly with these NPs. It is supposed that the antimicrobial effect of CuO NPs depends on the production of $\bullet O_2^-$ ROS [135]. However, Cu_2O is considered to be the more effective agent, forming a copper(I)-peptide complex; the inactivation of proteins caused by Cu_2O NPs cannot be detected when using CuO NPs [136]. Although CuO NPs can generate ROS while Cu_2O cannot, the antimicrobial efficacy of Cu_2O is, nonetheless, greater [136]. This conclusion may be evidence for the contact kill mechanism, as ROS do not work as efficiently as copper(I)-induced protein inactivation. Although CuO NPs also have antimicrobial properties when compared with Ag and Cu NPs, higher concentrations are required to attain the same antimicrobial efficacy [137,138]. In general, preventing oxidation is an efficient way to enhance the antimicrobial properties of Cu NPs.

4.4. Other Derivative NPs

Apart from oxide NPs, the main Ag-derived NPs are AgX (X = Cl, Br, I). Many studies posit that the antimicrobial mechanism of AgX NPs is related to their photocatalytic activities [139–141]: it was reported that AgBr NPs can form electron/hole pairs when irradiated with visible light at 400 nm, which may induce ROS production [142]. Another study posited that the antimicrobial behavior of AgCl and AgI NPs is based on the release of Ag ions, not noticeably different from antimicrobial Ag NPs [143]. However, because of their photocatalytic properties, AgX NPs are unstable under visible light irradiation, which results in the decline of their antimicrobial behavior over time [144]. Antimicrobial activities have also been reported for other Ag-related NPs, such as Ag_2S [145] and Ag_2Se [146].

In addition to Cu oxide, CuS [147] is the main Cu-based NP; it, too, displays antimicrobial behavior. It was found that CuS NPs, at specific wavelengths (980 nm [148] and 808 nm [149]), have strong photothermal effects, which can be used to kill bacteria. However, another study demonstrated that CuS NPs possess higher antimicrobial potency than Cu ions in the absence of light irradiation [150]. CuS-damaged cell walls were detected, because bacteria do not evolve to be resistant to membrane-disrupting antibiotics [151].

4.5. Bacterial Susceptibility

Different bacteria show different susceptibilities to Ag and Cu NPs. It was found that these NPs have equal antibacterial behavior toward Gram-positive bacteria [152]. A similar conclusion was obtained in another study, where *B. subtilis*, a Gram-positive

bacterium, had approximately equal sensitivity to both Ag and Cu NPs, although Cu NPs demonstrated a higher antimicrobial efficacy to the Gram-negative *E. coli* [153]. However, the opposite results were obtained in another report, which revealed that Ag NPs were more effective toward *E. coli* and *S. aureus*, while Cu NPs showed better antimicrobial action toward *B. subtilis* [115]. Similar results concluded that Cu NPs are more effective to the Gram-positive *B. subtilis*, while Ag NPs have superior antimicrobial activity against the Gram-negative *E. coli* [154]; thus, one cannot formulate an exact conclusion based on a comparison between Ag and Cu NPs toward different bacteria.

Some types of bacteria are resistant to Ag and/or Cu [155–157]. Cu-resistant bacteria exist extensively in Cu-contaminated soil [158,159]. One kind of Gram-positive bacterium, *Ent. faecium*, showed strong resistance to both Ag and Cu ions, probably because bacterial cellular Cu homeostasis resulted in Ag efflux [160]. However, the Gram-negative Cu-resistant bacterium, *E. coli*, is sensitive to Ag, the mechanism of which may be different from that of *Ent. faecium* [160]. Another study proposed nine genes in three transcription units, which could cause *Salmonella* resistance to Ag compounds [161]. A similar viewpoint proposed that Ag-resistant *E. coli* had a reduced outer membrane permeability, which was presumably determined by a chromosomal gene [162].

4.6. Cytotoxicity to Human Cells

NPs can release ions, induce intracellular ROS generation, or directly interact with cells, all of which are likely to cause cytotoxicity to human cells. In addition, the accumulation of toxic NPs in the environment would increase the possible environmental risk. Thus, the potential cytotoxicity of NPs to human must also be considered.

It is believed that Ag and Cu ions released into the environment are toxic to the human liver, kidney, eye and skin [163,164]. Generally, the cytotoxicity of NPs to human cells is also related to NP size, since NPs with large surface to volume ratios release more ions than bulk metals [165]. Apart from ions, an increasing amount of intracellular ROS induced by NPs may trigger cells death [166]. The ROS bursts and pro-inflammatory pathways induced by Ag NPs may lead to DNA damage, protein misfolding, and lipid peroxidation, all of which are possibly unrepairable, and potentially carcinogenic [167]. The effect of Ag NPs on the immune system should be further studied, since one report suggested that Ag NPs exerted cytotoxicity on macrophages, and resulted in an inflammatory response and cellular apoptosis [168]. Unlike Ag, Cu is a necessary element for the human body, where it must be retained in homeostasis. If the Cu content increases to break the equilibrium, it becomes toxic [169].

However, a histological study indicated that Ag and Cu NP coatings on catheters do not irritate the human skin [170]. It was also found that Ag-functionalized polyurethane is toxic to bacteria, but not to cells, when the Ag NP content is optimized to 0.5 wt %, at which cells vitality is near 100% [171]. This is attributed to the serum protein albumin in the cell culture medium, which reduces the biological interaction of the NPs with the cells [171]. The restraint to NPs by the immune system can result in a greater resistance of human cells, compared to microbes, to Ag NPs, which suggests that Ag NPs, at antibacterial concentrations, may be nontoxic to human cells [172]. It was also reported that newly produced Ag NPs are less toxic to human cells than older ones [173]. Immobilizing NPs can reduce their toxicities, compared to free NPs [174]. Titanium substrates, coated with chitosan, hydroxyapatite, and Ag NPs, revealed strong antimicrobial capacities and weak cytotoxicity to humans, since chitosan immobilizes Ag NPs firmly, thereby reducing cytotoxicity to human cells [175].

5. Coatings on Substrates

Besides being used as aqueous disinfectants [176,177], the main application of NPs is as coatings on substrates, such as textiles (synthetic polymers and cotton) and implants (polymers, ceramics and metals). Other products, including food packaging materials [178,179], and water [180,181] and air [182,183] filters, can also be decorated with antimicrobial NPs.

5.1. Coatings on Textiles

The COVID-19 pandemic has motivated work on antimicrobial NP-functionalized textiles, especially for use as face masks and protective clothing. Although the antiviral properties of Ag and Cu NPs are not clear, the NP decoration can improve the protective function of these masks [184]. N95 masks, impregnated with Cu oxide NPs, were reported to filter 99.85% of aerosolized viruses, such as human influenza A virus (H1N1) and avian influenza virus (H9N2), without reducing physical filtration performance [185]. In addition to viruses, textiles are common substrates for bacterial growth, under proper temperature and humidity condition [186]. Those impregnated with Ag and Cu NPs had dramatically enhanced antibacterial properties when compared to unimpregnated PET textile [187]. Similarly, studies on cotton textiles impregnated with Ag NPs, and those impregnated with a mixture of Ag and Cu NPs, both exhibited excellent antibacterial and antifungal properties [188]. It was initially hypothesized that the antimicrobial properties are dependent on both the textile and the NP [189], although it was subsequently demonstrated that the antimicrobial efficacy has nothing to do with the textile type, but depended only on the NPs [190].

Many methods of coating onto textiles have been reported. For instance, NP dispersions can be coated onto cotton fibers by means of pad dyeing [132], immersing [191], or ironing [190], all of which are traditional coating methods in the textile industry. Chemical reduction [192] is another commonly used treatment method: Ag and Cu NPs can be deposited onto PDA/PET fabrics by the chemical reduction of aqueous Ag and Cu salt solutions [187]. However, the problem for NPs loaded onto textiles is that they are poorly bonded, and tend to fall off during washing, leading to the loss of antimicrobial properties.

5.2. Coatings on Implants

Compared to the research on textiles, NP-functionalized implants (polymers, ceramics and metals) intended for the human body, must meet stricter standards of biocompatibility and biotoxicity.

Polyurethane is one of the most frequently used polymers in the biomedical field. It has been reported that polyurethane catheters can be Ag- and Cu-functionalized by sputtering, boosting its antimicrobial properties [116]. In addition to polyurethane, polyethylene is usually used in joint arthroplasty, owing to its remarkable mechanical properties, though it is easily attacked by microbes. In a study on polyethylene surface modifications, polyethylene coated with Ag NPs possessed greater antimicrobial properties than that coated with Cu NPs [193], which corresponds to the antimicrobial comparisons between Ag and Cu NPs discussed earlier. Other polymers, such as polytetrafluoroethylene (PTFE), used as an implant due to its good chemical resistance and thermal stability, were also coated with Ag and Cu NPs to improve their antimicrobial properties [194].

Bio-ceramics include bioinert, bioactive, and biodegradable ceramic materials. Bioinert ceramics are nontoxic, and do not interact with human tissue. Bioactive ceramics, such as bio-glass and hydroxyapatite, generate new bonds to human tissue. Biodegradable ceramics, such as calcium phosphates, are resorbed by the human body [195]. Here, we discuss bioinert ceramics, such as TaN, TiO_2, etc. Tantalum nitride (TaN), modified with both Ag and Cu NPs, displayed greater antimicrobial activity than either TaN-Ag or TaN-Cu, because of the synergistic effect of Ag and Cu NPs [196]. Another study reported that Cu NP-functionalized TiO_2 substrates do not exhibit antimicrobial activity, whereas both Ag NPs and AgCu alloy NPs show excellent antimicrobial properties, attributed to a substantially lower release of Cu ions [197].

Titanium (Ti) metal is widely used for orthopedic and dental implants. It was hypothesized that Ti substrates embedded with Ag NPs have enhanced electron transfer between Ag and Ti, which generates ROS to kill microbes [80]. It was noticed that, in some cases, Ti substrates were treated to form TiO_2 [197], or coated with hydroxyapatite [175], before further modification with NPs, in order to form porous surfaces that more firmly immobilized NPs.

Stainless steel is another metal used for medical applications, because of its distinct mechanical and corrosion-free features. Functionalized with Ag NPs, stainless steel showed stable antimicrobial activity, even over seven cycles of bacterial application [198]. Stainless steel, functionalized in this manner, was found to have not only bactericidal properties, but also resistance to bacteria adhesion [49].

Magnesium and its alloys are also potential implant materials. Magnesium may be intrinsically weakly toxic to microbes, since its corrosion creates an alkaline product [199]. In order to improve the antimicrobial property of magnesium, Cu NPs were coated onto its surface [200].

5.3. Surface Coating Methods on Implants

Various methods have been used to functionalize implants, including physical, chemical, and plasma depositions.

Magnetron sputtering is one of the widely used physical deposition methods, which results in uniform thickness, as well as strong bonding to substrates [201]. This method is generally used to produce thickness-controlled NP coatings [202]. An interesting study indicated that longer sputtering times are associated with enhanced cytotoxicity [203]. Hence, the determination of an optimal sputtering time is indispensable.

Chemical reduction on the substrate surface is the simplest and most widely used method. Ag NPs, depositing on the substrates, can be formed through the chemical reduction of metal salt solutions, which is similar to the functionalization of fabrics, described above, although the bond strength between NPs and these substrates is not high [201]. Reduction can be triggered by chemical agents [204,205], UV irradiation [206], etc. The antimicrobial properties of Ag NPs are enhanced with increased Ag salt solution concentrations [207]. It was found that the sequence of adding Ag salt solution and reducing agent influences the uniformity of surface modification [119], and may play a role here, too.

Plasma immersion ion implantation (PIII) is the most economical and effective, and involves positive ions vertically incorporating into a negatively charged surface under an electric field [208]. Thus, NPs can be impregnated into the near-surface of implants, including polymers, ceramics and metals [201]. The average size of Ag NPs incorporated into substrates increased with increased PIII time [198,209], because of aggregation. However, PIII was found to reduce Ag NP cytotoxicity by constraining NP mobility on titanium substrates [210].

Plasma electrolytic oxidation (PEO), also called micro-arc oxidation (MAO), is another commonly used plasma deposition method. PEO developed from anodization, forms ceramic-like coatings on substrates, which can tightly immobilize NPs onto surfaces [211]. PEO is often used to generate a porous titanium dioxide thin layer on titanium or titanium alloys, for further surface modification with NPs [212,213]. Magnesium alloys, implanted with Cu NPs through PEO, inhibited bacterial proliferation more efficiently than the alloy treated by PEO without Cu NPs [200].

Table 1 summarizes methods of implant surface modification with Ag NPs, Cu NPs, Ag–Cu NP mixtures, and AgCu nanoalloys. As can be seen, PIII is generally used to functionalize NPs on metals and polymers, while magnetron sputtering is usually employed for the surface modification of ceramics and polymers. Compared to PIII and magnetron sputtering, PEO can generate much thicker porous oxide layers, incorporated with NPs, on metal substrate surfaces. Since polymeric materials may contain various active functional groups, chemical reduction is not suggested for their modification. Apart from these, other surface functionalization methods, such as heating organic solvents [194], anodization [206], adding linkers on substrates [214], and electrodeposition [215], have been reported.

Table 1. Summary of implant surface modifications by Ag NPs, Cu NPs, Ag–Cu NPs mixture, and Ag–Cu nanoalloys.

Method	Substrate	NPs	Size (nm)	Coating Thickness (nm)	Application	Reference
Plasma immersion ion implantation (PIII)	Stainless steel	Ag NPs	5–16	Unknown	Implants	[198]
	Titanium	Ag NPs	Unknown	80	Implants	[80]
		Ag NPs	4–19	25	Implants	[209]
		Ag NPs	5–40	Unknown	Dental implants	[210]
		Ag NPs	5	50	Implants	[216]
	Polyethylene	Ag NPs, Cu NPs	Unknown	Unknown	Joint implants	[193]
Magnetron sputtering	Titanium dioxide	Ag NPs	14–42	Unknown	Coating	[90]
		Ag NPs	Unknown	24.6–73.8	Coating	[203]
	Tantalum nitride	Ag NPs, Cu NPs, Ag–Cu NPs mixture	Unknown	100	Coating	[196]
		Ag NPs	10–200	700	Coating	[217]
	Tantalum oxides	Ag NPs	<160	600–700	Coating	[218]
	Titanium-aluminum-nitride	AgCu nanoalloys	20–1100	100	Coating	[219]
	Polyether-ether-ketone	Ag NPs	Unknown	3–12	Implants	[202]
	Polyurethane	Ag–Cu NPs mixture	<5	Unknown	Catheter	[116]
		Ag–Cu NPs mixture	Unknown	80	Catheter	[170]
		Ag–Cu NPs mixture	Unknown	22	Catheter	[220]
Plasma electrolytic oxidation (PEO)	Titanium alloy	Ag NPs Cu NPs Ag–Cu NPs mixture	7–60	Unknown	Implants	[197]
		Ag NPs	37	Unknown	Implants	[212]
	Magnesium alloy	Cu NPs	Unknown	8000–11,000	implants	[200]
	Titanium	Cu NPs	Unknown	5000–10,000	Implants	[213]

Method	Substrate	NPs	Size (nm)	Coating Thickness (nm)	Application	Reducing Agent	Reference
Chemical reduction	Titanium dioxide	Ag NPs	102	Unknown	Coating	NaOH	[119]
		Ag NPs	600–1000	Unknown	Coating	Dehydrated ethanol	[205]
		Ag NPs	10–30	Unknown	Coating	Ammonia	[206]
		Ag NPs	20	Unknown	Coating	Glucose	[221]
	Titanium	Ag NPs	3–5	Unknown	Implants	UV&Methanol	[207]
		Ag NPs	30	Unknown	Implants	Ascorbic acid	[222]

6. Mixed Ag–Cu NPs and AgCu Nanoalloys

Although both Ag NPs and Cu NPs exert significant antimicrobial properties, mixtures of Ag and Cu NPs exhibit greater antimicrobial properties than either individual Ag or Cu NPs [196], which indicates the existence of synergistic antimicrobial behavior [197,223]. The mechanism of this synergy has been studied through a consideration of the nanocrystalline

microstructures formed. In this section, the synthesis of AgCu nanoalloys, microstructure, and physicochemical characterization, as well as the synergistic antimicrobial mechanism, are discussed.

6.1. Synthesis of AgCu Nanoalloys

The most conventional AgCu nanoalloy synthesis method is through the chemical reduction of a solution containing both Ag and Cu salts. Nanoalloys were synthesized from a solution of $AgNO_3$ and $CuSO_4$, using natural reducing agents, such as fruit peel extract [224], or Azadirachta indica leaf extract [225], as well as synthetic reducing agents, such as polyvinylpyrrolidone [9], polyol [226,227], ascorbic acid [228], dextrose [229], sodium borohydride [190], or tartaric acid [152]. Another study used oleyl amine as both reducing agent and surfactant, to synthesize nanoalloys from a solution of Ag and Cu(I) complexes, which gave a randomly distributed AgCu solid solution [230]. The chemical reduction method is also used to synthesize AgCu nanoalloys with the microstructure of either $Ag_{core}Cu_{shell}$ or $Cu_{core}Ag_{shell}$, depending on the sequence of reduction reactions [231].

Dealloying is another widely used synthesis method. It was found that a AgCu core-shell microstructure could be generated by dealloying a Zr-Cu-Ag-Al-O crystalline composite: Zr, Al and their oxides were dissolved, leaving Ag on the Cu surface [232]. Besides core-shell microstructures, single-phase supersaturated AgCu nanoalloys were synthesized through the dealloying of Ma-(Ag, Cu)-Y metallic glass precursors in H_2SO_4 [233,234].

Laser ablation is also a commonly used synthesis method. Nanosecond laser pulses, at specific wavelengths, were used to generate NPs [194]. It was reported that AgCu nanoalloys could be synthesized by irradiating an unfocused laser (800 nm) on a Ag and Cu colloidal solution for a period of time, while stirring [235]. Another study used a 1064 nm laser beam to irradiate pure Ag and Cu targets in an aqueous medium, adding different concentrations of capping agent to synthesize AgCu nanoalloys having different sizes [236]. AgCu nanoalloys having different compositions have also been synthesized by laser ablation [237].

The use of galvanic displacement reactions is an effective method to synthesize AgCu nanoalloys, especially for core-shell microstructures [238]. Galvanic displacement permits Ag precursors to chemically decompose, transferring electrons from Ag ions to Cu^0, replacing crystalline Cu atoms [239], ultimately forming Ag-doped AgCu nanoalloys. Another example, using a displacement reaction to synthesize AgCu nanoalloys, was based on the metallic activity difference between Ag and Cu, the first step of which is Cu NP generation from a Cu precursor, and the second step is Ag atom displacement of Cu atoms on the surface of Cu NPs through electrons transfer [240]. CuO microparticles, decorated with Ag NPs via galvanic displacement reactions, were also reported [241].

In addition to these methods, other synthesis approaches have been described, such as the sol-gel reaction [242], carbothermal shock [243], inert gas condensation [244], the electric explosion of twisted Ag and Cu wires [245], a core-shell structure produced by sono- and electrodeposition [246,247], and magnetron sputtering [248].

6.2. Microstructures of Mixed Ag–Cu NPs and AgCu Nanoalloys

Mixtures of bimetallic nanoparticles may form different microstructures (Figure 9) [249,250]. Segregated microstructures, with two or more separated NP clusters sharing a limited interface, include core-shell (Figure 9a), multi-shell (Figure 9b), and biphasic (Figure 9c) microstructures. Core-shell microstructures commonly exist in bimetallic NPs. In addition to segregated microstructures, mixed microstructure may be divided into an intermetallic structure (Figure 9d) with an ordered bimetallic atoms alignment, and a nanoalloy structure (Figure 9e) with randomly distributed bimetallic atoms [250].
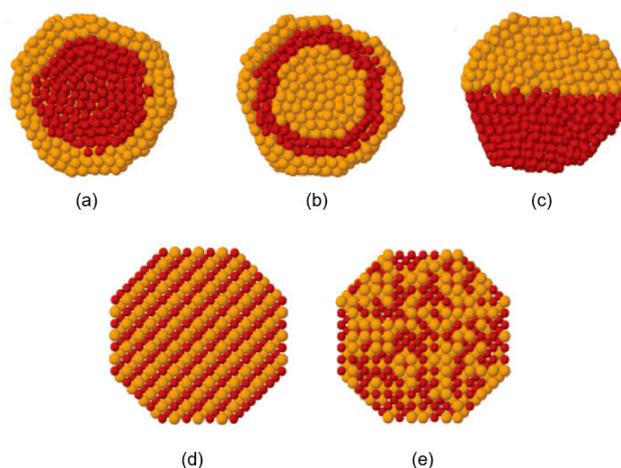
**Figure 9.** Microstructures of bimetallic NPs. (**a**) core-shell structure; (**b**) multi-shell structure; (**c**) biphase structure; (**d**) intermetallic structure; (**e**) nanoalloy. Reproduced with permission from Reference [249]. Copyright 2008, American Chemical Society.

As the Ag–Cu phase diagram indicates (Figure 10) [251], the metals are mutually immiscible at low temperature. Thus, mixed Ag and Cu bimetallic NPs generally form distinct phases [227,252], rather than homogeneously dispersed microstructures, as does the AuCu nanoalloy [253]. It has been reported that the Ag–Cu mixture tends to form core-shell structures, in which Ag is the shell and Cu the core. This is because Ag, with a lower surface energy (1.25 J/m^2) segregates on the surface of Cu NPs, with their greater surface energy (1.79 J/m^2) [190]. In an approximate sense, a mixture of Ag and Cu bimetallic NPs, with a nanograin microstructure, can be considered a single-phase nanoalloy (Figure 11a), whereas, in other microstructures, such as in Figure 11b,c, the Ag and Cu atoms do not distribute uniformly. It was found that homogenous AgCu nanoalloys (Figure 11a) gradually separate phases (Figure 11b–d), as the temperature is increased [254]. In addition to the influence of temperature, the morphologies of the Cu-rich α phase and the Ag-rich β phase can change with an increase of Cu content, passing from separated phases to nanograins to core-shell microstructures (Figure 12a–d), since the microsystems tend to keep the α-β interphase surface energy minimum [237,255]. In a broad sense, all the microstructures described here belong to AgCu nanoalloys, while only the simply mixed Ag–Cu system, without any combination reaction, is not so regarded.
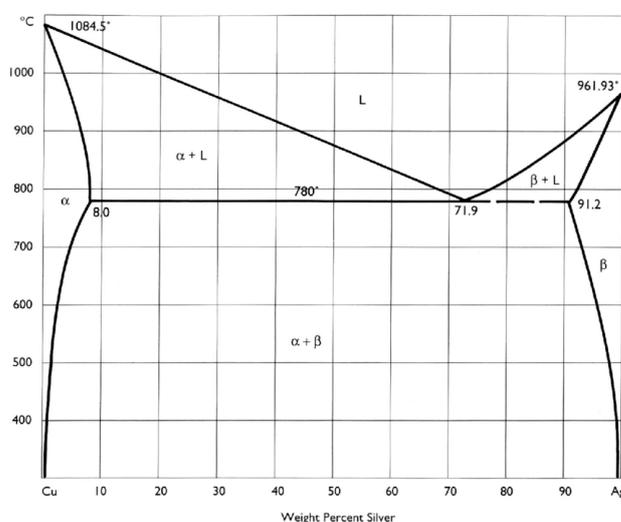
Figure 10. Ag–Cu phase diagram. Reproduced with permission from Reference [251]. Copyright 1991, J. Paul Getty Trust.
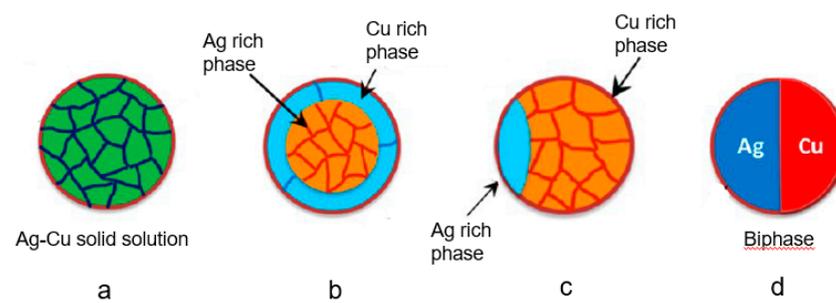
Figure 11. (**a**) Single-phase AgCu solid solution; (**b**) core-shell structure of AgCu nanoalloys; (**c**) structure of Ag and Cu in both phases; (**d**) biphasic. Reproduced with permission from Reference [254]. Copyright 2016, American Chemical Society.
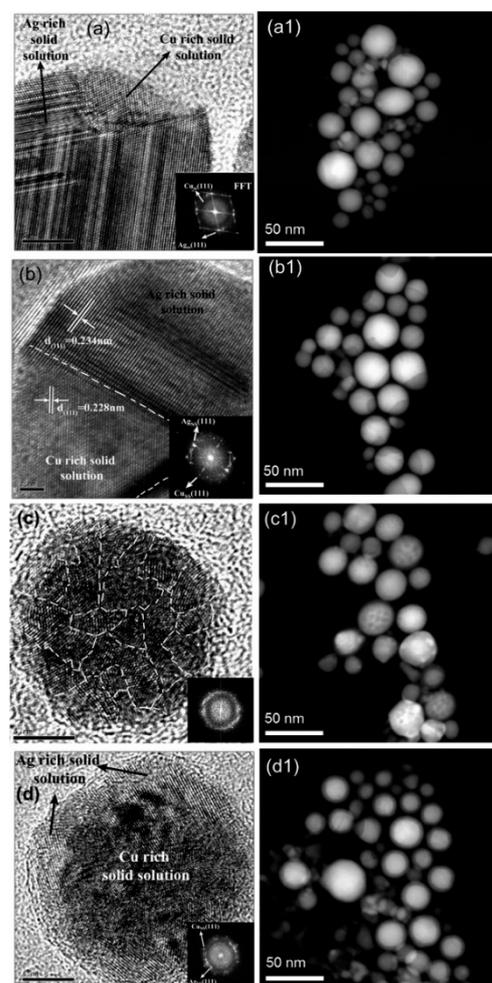
Figure 12. HRTEM photomicrographs of AgCu nanoalloys, showing four different microstructures: (**a**,**b**) separated phases, (**c**) nanograins and (**d**) core-shell with, respectively, four different Cu concentrations (20%, 40%, 60%, 80%). (**a1**–**d1**) images of four respective target compositions at low magnification. Reproduced with permission from Reference [237]. Copyright 2014, American Chemical Society.

For AgCu nanoalloys with nanograin microstructures, Ag atoms are doped into the grain boundaries of the Cu matrix, and vice versa. In the case of a doped Cu matrix [256], a hybrid Monte Carlo/molecular dynamics simulation showed that Ag atoms segregated in the grain boundaries between Cu crystals. Ag atoms gradually aggregated along grain boundaries as the Ag concentration was increased (Figure 13a,b). After exceeding the

threshold (50 atoms/nm^2), Ag atoms formed wetting nanolayers along the grain boundaries (Figure 13c–e). The reason is that these wetting nanolayers have lower energies [256]. In a similar fashion, when Cu atoms dope Ag, hybrid Monte Carlo/molecular dynamics simulations indicated that they segregated in grain or twin boundaries (Figure 14) [257].
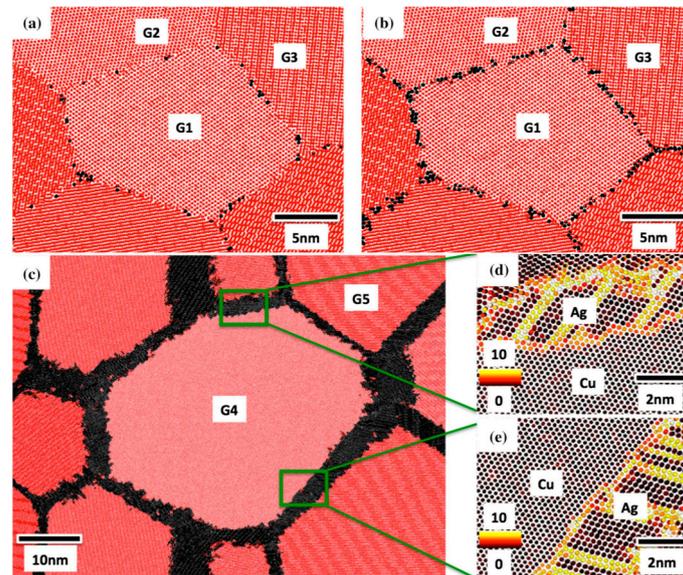
Figure 13. Microstructures of Ag doping Cu grain boundaries; (**a**–**c**) samples are based on the increases in Ag concentration; (**d**,**e**) are the Cu/Ag interfaces. For (**a**–**c**), red denotes Cu and black denotes Ag; for (**d**,**e**), the perfect FCC structure is marked 0, the light color, while defects are marked 10, the black color. Reproduced with permission from Reference [256]. Copyright 2017, Springer Nature.
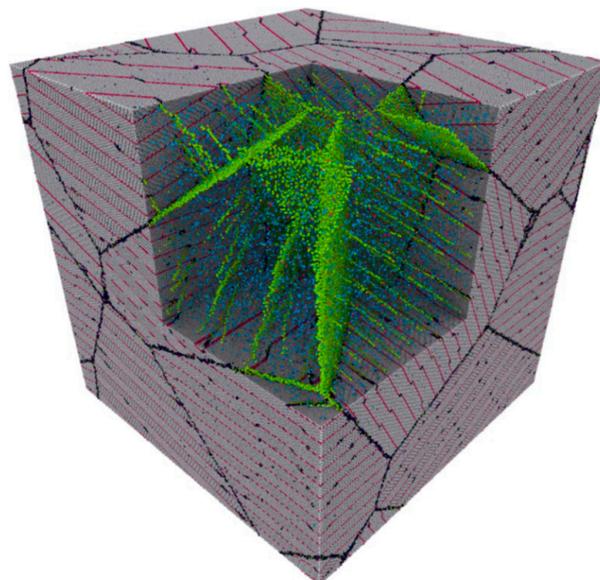
Figure 14. Simulated microstructure of Cu atoms doping Ag grain and twin boundaries; green represents Cu. Reproduced with permission from Reference [257]. Copyright 2019, Springer Nature.

## 6.3. Physicochemical Characterizations

It is clear that the NP surface plays an important role in its antibacterial behavior. For this reason, research on NP surface properties appears to be a key direction, particularly in determining their compositions, and how they might contribute to the antimicrobial behav-

ior. Hence, physicochemical characterization approaches are commonly used, including TOF-SIMS, XPS, TEM, SEM, EDXS, XRD, nanoIR® (Bruker, Billerica, MA, USA), etc.

6.3.1. TOF-SIMS and XPS

Time-of-flight secondary ion mass spectrometry (TOF-SIMS) [258,259] is an appropriate characterization method for NP surface analysis. It detects fragments sputtered from the surface. It has a probe depth of ≤1 nm and can sensitively detect fractional layers of surface components. Hence, it is possible to use TOF-SIMS to determine which chemical groups exist on the surfaces of NPs, and which component is the most effective antimicrobial agent.

Another surface characterization technique, X-ray photoelectron spectroscopy (XPS) [260,261] can be used to determine chemical environments and oxidation states of elements on the surfaces of NPs. While less surface-sensitive than TOF-SIMS (it has a probe depth of 3–5 nm, depending on the kinetic energy of the emitted electron), it can detect whether Ag and Cu NPs have been oxidized, and which oxides have been produced.

Since XPS can detect element quantitatively, the surface composition of AgCu is approximately equal to the area ratio of $Ag3d_{5/2}$ to $Cu2p_{3/2}$ spectra, which are the most prominent spectral peaks of these elements [8]. XPS also indicated that, for both Ag and Cu NPs deposited onto the surface of polyurethane, Cu^0 was found only at the surface of the AgCu nanofilm with an Ag:Cu ratio of 1:1, a ratio that exhibits the most efficient antimicrobial activity [116]. For $AgCu_2O$ nanoalloys (Figure 15), the major $Cu2p_{3/2}$ peak, at ~934 eV, indicates the presence of Cu^+, while the shake-up satellite indicates that some of it has been partially oxidized to CuO. The $Ag3d_{5/2}$ peak, at ~368 eV, indicates the presence of Ag^0 [242]. This indicates that Ag has formed a shell around partially oxidized Cu_2O.
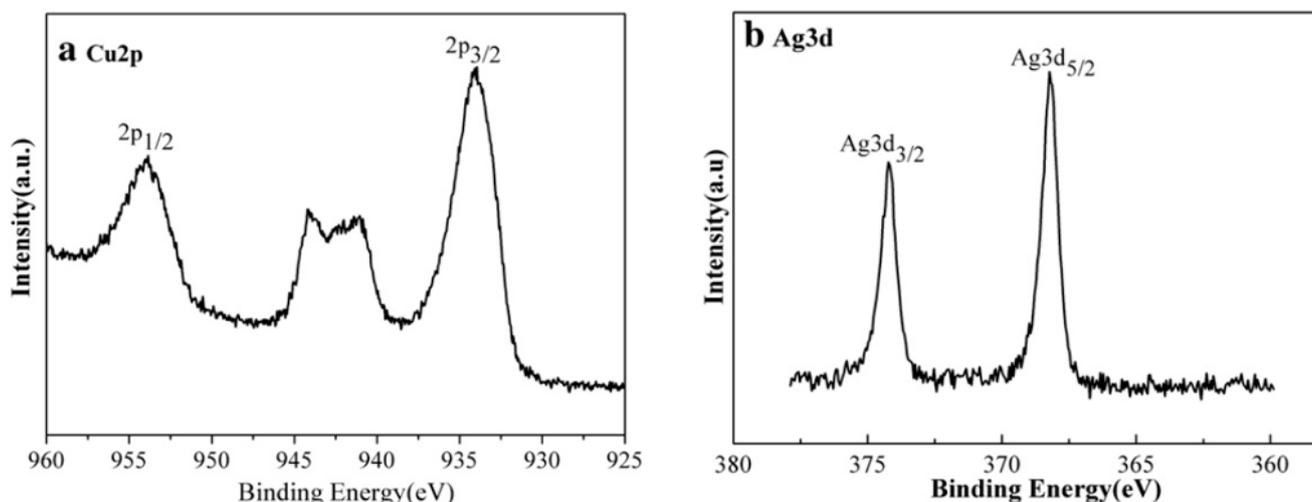
Figure 15. XPS spectra of (**a**) Cu2p and (**b**) Ag3d in $AgCu_2O$ nanoalloys. Reproduced with permission from Reference [242]. Copyright 2015, Elsevier.

Changing the XPS probe depth, by sputtering away the outer surface, can be used to identify the core-shell structures of nanoalloys. While the Cu shake-up satellite indicates the presence of CuO (Figure 16a), sputtering to a depth of 10 nm causes the satellite region to disappear (Figure 16b), which indicates the existence of CuO at the surface, rather than in the core. By contrast, Ag is not easily oxidized (Figure 16c). Moreover, the relative increase in the Cu:Ag ratio on sputtering reveals that, aside from CuO, Cu tends to occupy the core of the structure (Figure 16b,d) [262], as expected for a $Ag_{shell}Cu_2O_{core}$ structure.
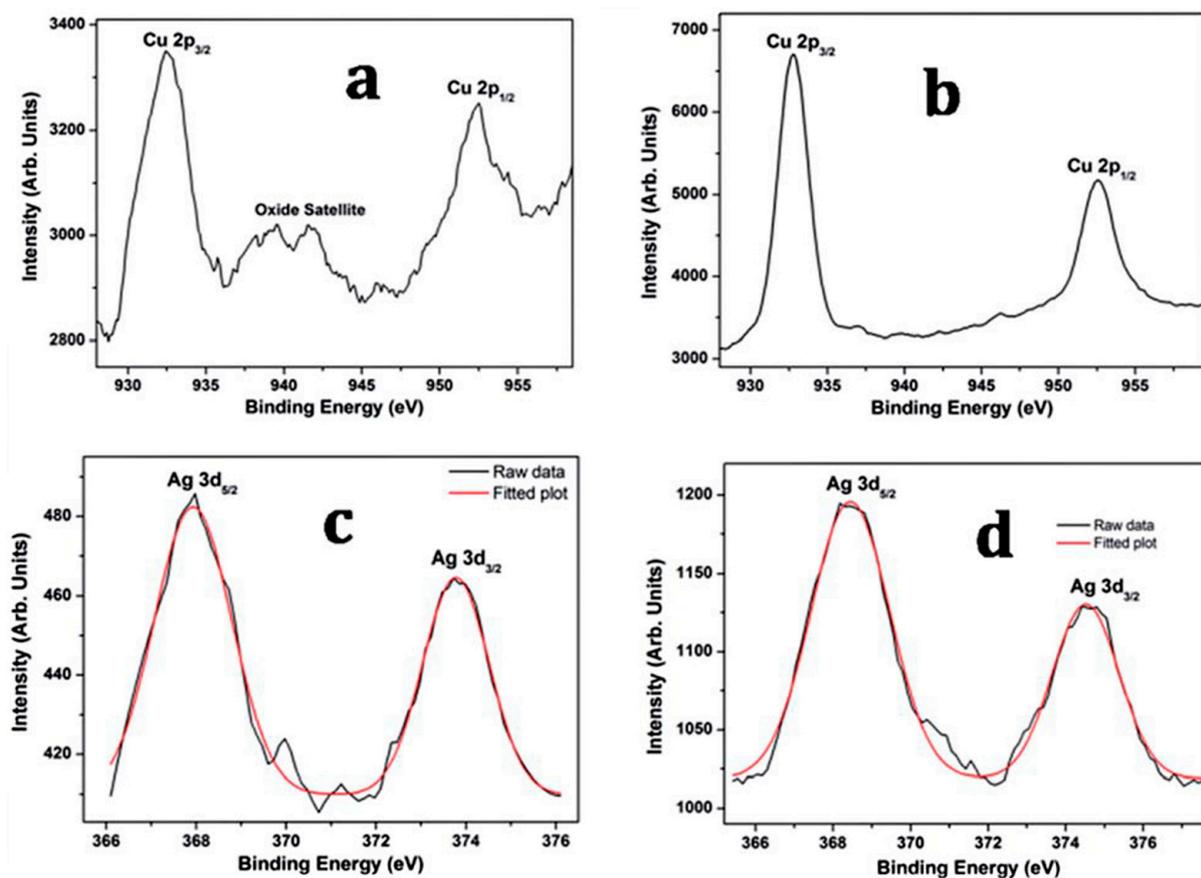
Figure 16. XPS spectra of Cu2p (**a**) before and (**b**) after sputtering, and Ag3d (**c**) before and (**d**) after sputtering, in Ag$_{shell}$Cu$_{core}$ nanoalloy. Reproduced with permission from Reference [262]. Copyright 2015, Royal Society of Chemistry.

Generally, TOF-SIMS is combined with XPS to investigate the chemical components more accurately, with one supporting the results of the other [81,263,264]. In one report, N was detected by TOF-SIMS, but not by XPS, which means N-containing species, at very low concentrations, are confined on the surface of Ag NPs [86]. Thus, TOF-SIMS can not only confirm the XPS results, but often provide more detail.

6.3.2. TEM and EDXS

Transmission electron microscopy (TEM) [265] is frequently used to observe NP morphologies and antimicrobial activities; high-resolution transmission electron microscopy (HRTEM or HREM) is a particularly informative imaging mode. TEM offers images of internal information such as crystal structure, morphology, and mechanical stress, with resolutions down to 50 pm. It is generally used to evaluate morphological features, such as NP sizes and shapes [112], or to observe the antimicrobial behavior of NPs penetrating into bacterial cell [266]. NP surface modification [132], as well as substrate decoration [127,267], can also be directly detected by TEM. It has been reported that both Ag and Cu NPs can induce cell wall separation from cell membranes, leading to the further damage of cell walls and membranes and, ultimately, cytoplasmic material release, all of which have been observed by TEM [111]. HRTEM can even provide the details of the nanocrystalline structure (Figure 12). As another example, the core-shell microstructures of AgCu nanoalloys, with different orientations of the crystal facets of Ag (2, 0, 0) and Cu (2, 0, 0), can be clearly observed via HRTEM (Figure 17) [268].
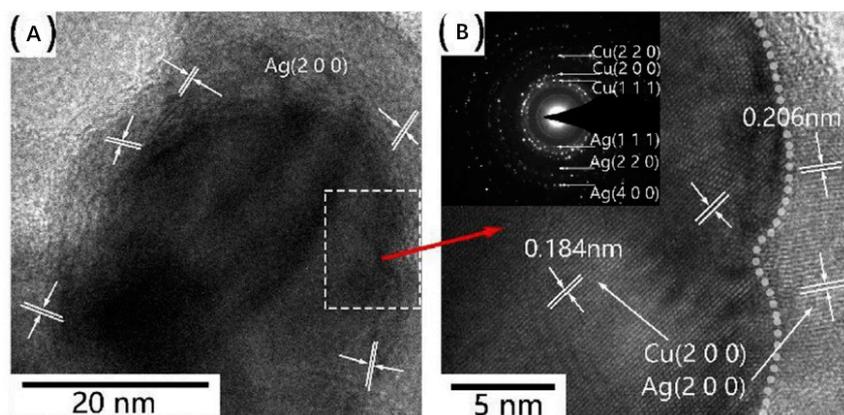
Figure 17. (**A**) HRTEM image of core-shell microstructure, in which Cu is the core, and Ag the shell; (**B**) magnified HRTEM image. Reproduced with permission from Reference [268]. Copyright 2017, Elsevier.

Energy-dispersive X-ray spectroscopy (EDS, EDX, EDXS or XEDS) [269] is a widely employed characterization technique, often used for elemental and chemical analyses. Commonly, EDXS is used with TEM, to obtain chemical proportions and distributions in NPs. TEM-EDXS spectra of AgCu nanoalloys provided the ratio of Ag and Cu, which was consistent with the initial ratio of Ag and Cu salt precursors [227]. Different microstructures, such as homogeneous nanoalloy and core-shell AgCu microstructures, can be distinguished by means of EDXS. EDXS chemical analysis indicated that Ag and Cu are well mixed in the AgCu nanoalloy, although the Cu content is higher in the shell and the Ag content in the core, of core-shell microstructure [190]. Another more comprehensive report of TEM-EDXS spectra, in the HAADF (high-angle annular dark field) mode, distinguished four different types of component distribution in AgCu nanoalloys (Figure 18) [237].
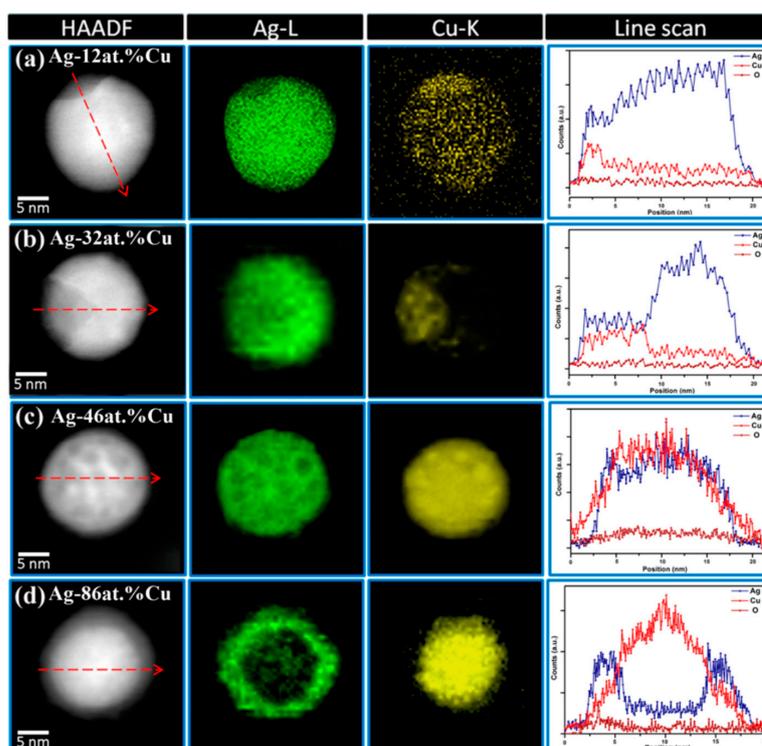

Figure 18. TEM-EDXS in high-angle annular dark field (HAADF) mode analysis of four different types of distribution of Ag and Cu in nanoalloy. Red arrow on HAADF image is the position and direction of line scan. Reproduced with permission from Reference [237]. Copyright 2014, American Chemical Society.

EDXS can also be used in combination with XPS: for a mixture of Ag and Cu NPs, XPS revealed that the Ag content was greater than that evaluated by EDXS. This was explained as follows: the act of mixing the Ag and Cu NPs formed a core-shell microstructure, with Ag at the surface [246].

6.3.3. XRD

X-ray diffraction (XRD) [270] is used to determine crystalline microstructure. When studying AgCu nanoalloys, it was used to determine whether the microstructure is a single phase or separated phases, through observing whether there is a shift of the diffraction peaks [242]. One study deduced that the microstructure was actually phase-separated instead of an alloy, because of the existence of distinct diffraction peaks of both Ag and Cu in mixed Ag–Cu NPs (Figure 19) [246]. A second study, on Cu_2O-Ag nanocomposites, reached a similar conclusion [271]. If Ag and Cu formed a homogeneously distributed nanoalloy microstructure, the diffraction peaks of Cu and Cu oxides would not appear in the XRD (Figure 20a,b) [272]. On the contrary, the presence of the diffraction peaks of Cu and Cu oxides in the spectrum indicated that the phases are separated (Figure 20c,d) [272]. The formation of oxide-free AgCu nanoalloys can also be determined by XRD, through the absence of the CuO diffraction peak at 61.7° and the Cu_2O diffraction peak at 37.5° [227].
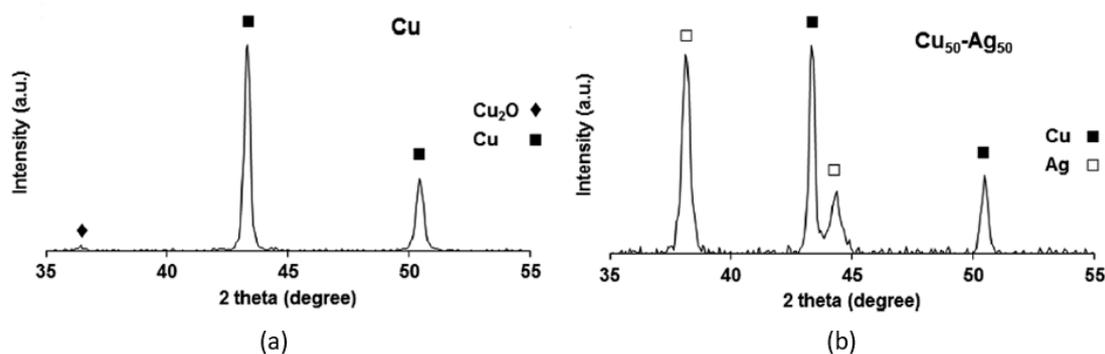
Figure 19. XRD spectra of (**a**) Cu NPs and (**b**) Cu_{50}-Ag_{50} NPs. Reproduced with permission from Reference [246]. Copyright 2016, Royal Society of Chemistry.
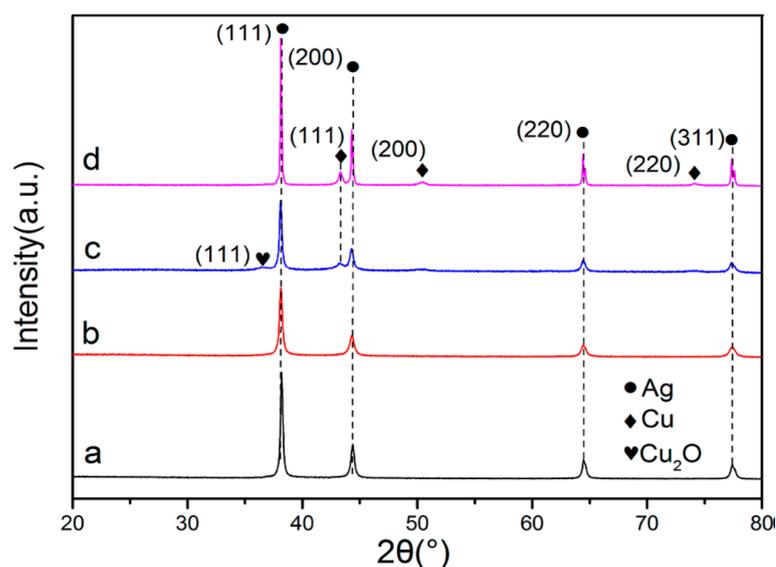
Figure 20. XRD spectra: (a) no Cu peaks in the spectrum of Ag_6Cu; (b) no Cu peaks in the spectrum of Ag_2Cu; (c) peaks of Cu and Cu_2O in the spectrum of $AgCu_3$; (d) peaks of Cu and Cu_2O in the spectrum of $AgCuO_x$. Reproduced with permission from Reference [272]. Copyright 2019, American Chemical Society.

6.3.4. Other Characterization Techniques

NanoIR® [273,274] is a new technique, which has a great potential to analyze NPs. Conventional IR technology provides information on functional groups, whereas atomic force microscopy (AFM) offers information on surface morphology. It is common to use both IR and AFM to evaluate NPs [29,117,132,154]. In contrast, nanoIR® possesses these two functions simultaneously, although no research group appears to have yet used it to analyze NPs.

In addition to the characterization methods above, thermal analyses (i.e., TGA and DSC) [275], surface-enhanced Raman spectroscopy [276], and UV-vis spectroscopy [277] have also been used to study the antimicrobial behavior of NPs.

6.4. Antimicrobial Potential of Mixed Ag–Cu NPs and AgCu Nanoalloys

AgCu alloys, clad as millimeter-thick coating layers on stainless steel substrates, were found to exhibit high antimicrobial activity [278]. Unfortunately, the physicochemical and biological properties of mixed Ag–Cu NPs and AgCu nanoalloys are presently not clearly understood, even though their excellent antimicrobial activities are well known. A comparison is found, in Table 2, among Ag, Cu, mixed Ag–Cu and AgCu nanoalloy NPs. Because of different microstructures and Ag:Cu ratios, antimicrobial conclusions are not always identical.

Table 2. Summary of microstructures and antimicrobial properties of Ag–Cu combinations.

Microstructure	Size (nm)	Ratio (Ag:Cu)	Control NPs	Strain	Antimicrobial Efficacy	Reference
Unknown	200	1:1	Ag NPs Cu NPs Ag–Cu NPs	*E. coli* *B. subtilis*	AgCu > Ag > (Ag–Cu) > Cu	[11]
	30–55	3:1 1:1 1:3	Ag NPs Cu NPs	*E. coli* *S. aureus*	Cu > $AgCu_3$ > AgCu > Ag_3Cu > Ag	[126]
	2–5	1:1 2:1 3:1	Ag NPs Cu NPs	*E. coli*	AgCu > Ag_2Cu > Ag_3Cu > Cu > Ag	[116]
	20–30	1:1	Ag NPs	*E. coli* *K. pneumoniae* *E. aerogenes* *P. mirabilis* *P. aeruginosa* *S. aureus*	AgCu > Ag	[188]
				E. faecalis	Ag > AgCu	
	7–60	1:1 3:1	Ag NPs Cu NPs	*S. aureus*	AgCu ≈ Ag_3Cu > Ag > Cu	[197]
	20	1:1 3:1	Ag NPs Cu NPs	*E. coli*	AgCu > Ag_3Cu > Ag ≈ Cu	[233]
				S. aureus	AgCu > Ag_3Cu ≈ Ag ≈ Cu	
	215–788	1:1	Ag NPs Cu NPs	*S. aureus*	AgCu ≈ Cu > Ag	[279]
				K. pneumoniae	AgCu > Cu > Ag	
	Unknown	3:1 1:1 1:3	Ag NPs Cu NPs	*S. aureus*	Ag_3Cu > AgCu > Ag > $AgCu_3$ > Cu	[282]
	30–80	Unknown	Ag NPs Cu NPs	*E. coli*	AgCu > Ag or Cu	[281]
				P. aeruginosa		
				S. typhi		
	20–180	0.1:3 0.2:2 0.3:1	Ag NPs Cu NPs	*E. coli*	$Ag_{0.2}Cu_2$ ≈ $Ag_{0.3}Cu$ > $Ag_{0.1}Cu_3$ > Ag > Cu	[283]
				S. aureus	$Ag_{0.2}Cu_2$ is the best	

Table 2. *Cont.*

Microstructure	Size (nm)	Ratio (Ag:Cu)	Control NPs	Strain	Antimicrobial Efficacy	Reference
	3	1:1	Ag NPs Cu NPs	*E. coli*	$AgCu > Ag > Cu$	[284]
	500–600	Unknown	Cu NPs	*E. coli*	$AgCu > Cu$	[285]
				S. aureus		
Core-shell ($Ag_{Core}Cu_{shell}$)	20–70	1:1	Ag NPs Cu NPs $Cu_{Core}Ag_{shell}$ NPs	*E. coli*	$Ag_{core}Cu_{shell} > Cu_{core}Ag_{shell} > Ag > Cu$	[231]
				K. pneumoniae	$Ag_{core}Cu_{shell} > Cu_{core}Ag_{shell} > Ag > Cu$	
				P. aeruginosa	$Ag_{core}Cu_{shell} > Cu_{core}Ag_{shell} \approx Ag > Cu$	
				S. aureus	$Ag_{core}Cu_{shell} > Cu_{core}Ag_{shell} > Ag > Cu$	
				A. fumigatus	$Cu_{core}Ag_{shell} > Ag > Ag_{core}Cu_{shell}$	
	<100	22:78 65:35 94:6	Ag NPs Cu NPs	*E. coli*	$Ag_{65}Cu_{35} \approx Ag_{22}Cu_{78} > Ag_{94}Cu_6 > Ag \approx Cu$	[245]
				S. aureus	$Ag_{65}Cu_{35} \approx Ag_{22}Cu_{78} > Ag_{94}Cu_6 > Ag > Cu$	
Core-shell ($Cu_{Core}Ag_{shell}$)	1000–1500	1:10 1:5 3:10	Cu NPs	*E. coli*	$Ag_3Cu_{10} > AgCu_5 > AgCu_{10} \approx Cu$	[152]
				S. aureus	$Ag_3Cu_{10} > AgCu_5 > AgCu_{10} > Cu$	
	7	1:3 2:3 1:1 4:1	Cu NPs	*E. coli*	$Ag_4Cu > AgCu > Ag_2Cu_3 \approx AgCu_3 \approx Cu$	[246]
				S. aureus	$Ag_4Cu \approx AgCu \approx Ag_2Cu_3 \approx Cu > AgCu_3$	
				B. subtilis	$AgCu > Ag > (Ag\text{–}Cu) > Cu$	
	150	Unknown	Cu_2O NPs	*E. coli*	$Cu_2OAg > Cu_2O$	[242]
	400–500	Unknown	Cu_2O NPs	*S. aureus*	$Cu_2OAg > Cu_2O$	[271]
				P. aeruginosa		
	3000	Unknown	μCuO Ag NPs	*E. coli*	$\mu CuOAg > Ag > \mu CuO$	[241]
				Salmonella	$\mu CuOAg > Ag > \mu CuO$	
				Listeria	$CuO > CuO > Ag$	
	10–30	1:1 3:1 5:1	-	*E. coli*	$AgCu \approx Ag_3Cu \approx Ag_5Cu$	[286]
				S. aureus	$Ag_5Cu > Ag_3Cu > AgCu$	
				A. flavus	$Ag_5Cu > Ag_3Cu > AgCu$	
				C. albicans	$Ag_5Cu > Ag_3Cu > AgCu$	

Table 2. *Cont.*

Microstructure	Size (nm)	Ratio (Ag:Cu)	Control NPs	Strain	Antimicrobial Efficacy	Reference
Nanoalloy	35–50	Unknown	Ag NPs Cu NPs $Ag_{Core}Cu_{shell}$ NPs $Cu_{Core}Ag_{shell}$ NPs	*C. albicans*	Homogeneous AgCu > $Ag_{core}Cu_{shell}$ > Ag > $Cu_{core}Ag_{shell}$ > Cu	[22]
				E. coli	Homogeneous AgCu > $Cu_{core}Ag_{shell}$ > Cu	
				S. aureus	Homogeneous AgCu > Cu > Cu_{core}-Ag_{shell}	
	5–7	1:1	Ag NPs Cu NPs	*E. coli* *S. aureus*	AgCu > Cu > Ag	[224]
	2.1	1:1	Ag NPs Cu NPs biphase AgCu	*E. coli*	Homogeneous AgCu > phase-separated AgCu ≈ Ag > Cu	[280]
				S. aureus	Homogeneous AgCu > Ag > biphase AgCu > Cu	

Polyester fabrics, coated by mixed Ag–Cu NPs without specific microstructures, have shown significantly enhanced antimicrobial properties over Ag-treated fabrics [279]. Another example, which did not evaluate the AgCu microstructure, compared single Ag and Cu NPs, mixed Ag–Cu NPs, and AgCu nanoalloys, and concluded that the antimicrobial activity of AgCu nanoalloys is much greater than those of the other three [11]. Further, porous AgCu nanoalloys revealed much stronger antimicrobial activities to both Gram-positive and Gram-negative bacteria than either Ag or Cu NPs, when the Ag:Cu ratio was 1:1 [233]; changing the ratio decreased the activity. Another study found that a AgCu nanoalloy with the Ag:Cu ratio of 13:7 had the strongest antimicrobial activity, because it released the greatest amount of ions [245].

In the case of AgCu nanoalloys with core-shell microstructures, it was found that different Ag:Cu ratios demonstrated different antimicrobial efficacies, in which the mixture with a higher ratio (0.3) showed better antimicrobial activity than lower ratios (0, 0.1, 0.2) [152]. Similar conclusions was obtained in another study, which indicated that Ag and Cu NPs, in a core-shell microstructure, had excellent antimicrobial activities against both Gram-positive and Gram-negative bacteria, especially when the Ag:Cu ratio was 0.4 [246]. However, in the case of antifungal properties, $Ag_{core}Cu_{shell}$ nanoalloys were found not to demonstrate higher activity than single Ag NPs [231]. Another viewpoint holds that $Ag_{shell}Ag$–Cu_{core} nanoalloys have long-term antimicrobial activity because the Ag shell has excellent oxidative stability [232]. Additionally, CuO_2 NPs, combined with Ag NPs to form core-shell nanoalloys, exhibited higher antimicrobial action than did CuO_2 NPs [241,242]. However, the antimicrobial properties of core-shell AgCu nanoalloys were still lower than those of uniformly distributed AgCu nanoalloys, which may stem from weaker Ag–Cu interactions in core-shell structures [22].

It was suggested that the much stronger antimicrobial activity of Ag–Cu nanoalloys is due to the greater amount of released Ag ions [280]. According to this study, charge transfer exists only at the interface of phase-separated Ag and Cu, thereby causing a weak release of Ag ions, whereas Ag atoms, surrounded by Cu atoms, can be oxidized, releasing more ions. In contrast, it was suggested that the higher antimicrobial properties of AgCu nanoalloys were due to the much larger (28×) amount of Cu ions released from nanoalloys than from single Cu NPs [271,281].

Another study proposed that the proteins and enzymes of microbes are susceptive to either Ag or Cu, and that AgCu nanoalloys can provide both metals, which exhibit synergistic antimicrobial activity [224]. However, as indicated in the probable antimicrobial mechanisms discussed above, the release of ions may be neither the correct, nor the only, reason. It appears necessary to determine the specific kinds of ROS generated: for

example, titanate nanotubes, embedded with Ag and Cu NPs, showed much more effective antimicrobial activity than either Ag or Cu NPs, when under visible light radiation (Ag–Cu heterojunctions can reduce electron-hole recombination, and generate higher amounts of ROS, such as $\bullet O_2{}^-$ and H_2O_2) [282].

7. Conclusions and Perspectives

While the data reported are inconsistent, due, at least in part, to our ignorance in framing the studies so as to take all the variables into consideration, two conclusions seem obvious: first, the operative antimicrobial mechanism depends on the conditions under which the study was carried out; second, the antimicrobial efficacy follows the order, Ag NPs $\approx$ Cu NPs < mixed Ag–Cu NPs < AgCu nanoalloys.

The possible mechanisms discussed herein imply that dry NPs, their ions, and the ROS produced, all exert some antimicrobial effect. It is, therefore, difficult to distinguish which is the predominant mechanism under any given set of circumstances. It will be important for future studies to concentrate on specifically controlled experiments, to determine explicit details, such as which kinds of ROS are produced, and how NPs kill microbes under dry conditions without releasing ions.

Further, there is a synergy in using mixed Ag–Cu NPs, indicating that the antimicrobial modes of Ag and Cu NPs differ. In addition, the fact that antimicrobial properties of mixed Ag–Cu NPs are weaker than those of AgCu nanoalloys tells us there is something present in the AgCu nanoalloy that does not exist in the simple Ag–Cu mixture. Future work should focus on this synergy, and the relationship between the surface structures of AgCu nanoalloys and their antimicrobial action.

Author Contributions: Conceptualization, E.S. and L.Y.; methodology, X.F.; validation, E.S., L.Y. and X.F.; formal analysis, X.F.; data curation, X.F.; writing—original draft preparation, E.S. and X.F.; writing—review and editing, E.S and L.Y.; supervision, E.S.; project administration, L.Y.; funding acquisition, L.Y. All authors have read and agreed to the published version of the manuscript.

Institutional Review Board Statement: Not applicable.

Informed Consent Statement: Not applicable.

Data Availability Statement: No new data were created or analyzed in this study. Data sharing is not applicable to this article.

Conflicts of Interest: The authors declare no conflict of interest.

Appendix A

Table A1. Data examined in the Polytechnique Montreal library Compendex database.

Objective	Key Words
Cu	(antimicrob* OR antibact* OR biocid* OR antibiof* OR antivir* OR antifung*) AND (copper* OR Cu OR CuO OR CuNP* OR nanocopper OR nano-copper OR nanoCu OR Cu-*)
Ag	(antimicrob* OR antibact* OR biocid* OR antibiof* OR antivir* OR antifung*) AND (silver OR Ag OR AgNP* OR nanosilver OR nano-Ag OR nanoAg OR Ag-*)
Cu nano	(antimicrob* OR antibact* OR biocid* OR antibiof* OR antivir* OR antifung*) AND (copper nano* OR Cu NP* OR CuNP* OR Cu nano*)
Ag nano	(antimicrob* OR antibact* OR biocid* OR antibiof* OR antivir* OR antifung*) AND (silver nano* OR Ag NP* OR AgNP* OR Ag nano*)
Combination of Ag, Cu nano	(antimicrob* OR antibact* OR biocid* OR antibiof* OR antivir* OR antifung*) AND (silver-copper OR copper-silver OR Ag-Cu OR Cu-Ag OR silver/copper OR copper/silver OR Ag/Cu OR Cu/Ag OR Ag@Cu OR Cu@Ag OR AgCu OR CuAg) AND (nano* OR alloyed nano* OR nanoalloy* OR nano-alloy*)

* refers to the end of the syllables researched.

References

1. Li, Y.; Xiao, P.; Wang, Y.; Hao, Y. Mechanisms and Control Measures of Mature Biofilm Resistance to Antimicrobial Agents in the Clinical Context. *ACS Omega* **2020**, *5*, 22684–22690. [CrossRef]
2. Zhao, Y.; Jiang, X. Multiple strategies to activate gold nanoparticles as antibiotics. *Nanoscale* **2013**, *5*, 8340–8350. [CrossRef] [PubMed]
3. Lee, N.-Y.; Hsueh, P.-R.; Ko, W.-C. Nanoparticles in the treatment of infections caused by multidrug-resistant organisms. *Front. Pharmacol.* **2019**, *10*, 1153. [CrossRef] [PubMed]
4. Chernousova, S.; Epple, M. Silver as antibacterial agent: Ion, nanoparticle, and metal. *Angew. Chem. Int. Ed. Engl.* **2013**, *52*, 1636–1653. [CrossRef]
5. Chaloupka, K.; Malam, Y.; Seifalian, A.M. Nanosilver as a new generation of nanoproduct in biomedical applications. *Trends Biotechnol.* **2010**, *28*, 580–588. [CrossRef]
6. Le Ouay, B.; Stellacci, F. Antibacterial activity of silver nanoparticles: A surface science insight. *Nano Today* **2015**, *10*, 339–354. [CrossRef]
7. Hostynek, J.J.; Maibach, H.I. Skin irritation potential of copper compounds. *Toxicol. Mech. Methods* **2004**, *14*, 205–213. [CrossRef] [PubMed]
8. Taner, M.; Sayar, N.; Yulug, I.G.; Suzer, S. Synthesis, characterization and antibacterial investigation of silver–copper nanoalloys. *J. Mater. Chem.* **2011**, *21*, 13150–13154. [CrossRef]
9. Reyes-Blas, M.; Maldonado-Luna, N.M.; Rivera-Quiñones, C.M.; Vega-Avila, A.L.; Roman-Velázquez, F.R.; Perales-Perez, O.J. Single Step Microwave Assisted Synthesis and Antimicrobial Activity of Silver, Copper and Silver-Copper Nanoparticles. *J. Mater. Sci. Chem. Eng.* **2020**, *8*, 13–29. [CrossRef]
10. Azam, A.; Ahmed, A.S.; Oves, M.; Khan, M.S.; Habib, S.S.; Memic, A. Antimicrobial activity of metal oxide nanoparticles against Gram-positive and Gram-negative bacteria: A comparative study. *Int. J. Nanomed.* **2012**, *7*, 6003. [CrossRef]
11. Zain, N.M.; Stapley, A.; Shama, G. Green synthesis of silver and copper nanoparticles using ascorbic acid and chitosan for antimicrobial applications. *Carbohydr. Polym.* **2014**, *112*, 195–202. [CrossRef]
12. Feng, Q.L.; Wu, J.; Chen, G.; Cui, F.; Kim, T.; Kim, J. A mechanistic study of the antibacterial effect of silver ions on Escherichia coli and Staphylococcus aureus. *J. Biomed. Mater. Res.* **2000**, *52*, 662–668. [CrossRef]
13. Kim, J.S.; Kuk, E.; Yu, K.N.; Kim, J.-H.; Park, S.J.; Lee, H.J.; Kim, S.H.; Park, Y.K.; Park, Y.H.; Hwang, C.-Y. Antimicrobial effects of silver nanoparticles. *Nanomed. Nanotechnol. Biol. Med.* **2007**, *3*, 95–101. [CrossRef] [PubMed]
14. Ramage, G.; Mowat, E.; Jones, B.; Williams, C.; Lopez-Ribot, J. Our current understanding of fungal biofilms. *Crit. Rev. Microbiol.* **2009**, *35*, 340–355. [CrossRef]
15. Lara, H.H.; Ixtepan-Turrent, L.; Jose Yacaman, M.; Lopez-Ribot, J. Inhibition of Candida auris Biofilm Formation on Medical and Environmental Surfaces by Silver Nanoparticles. *ACS Appl. Mater. Interfaces* **2020**, *12*, 21183–21191. [CrossRef] [PubMed]
16. Xia, Z.K.; Ma, Q.H.; Li, S.Y.; Zhang, D.Q.; Cong, L.; Tian, Y.L.; Yang, R.Y. The antifungal effect of silver nanoparticles on Trichosporon asahii. *J. Microbiol. Immunol. Infect.* **2016**, *49*, 182–188. [CrossRef] [PubMed]
17. Panacek, A.; Kolar, M.; Vecerova, R.; Prucek, R.; Soukupova, J.; Krystof, V.; Hamal, P.; Zboril, R.; Kvitek, L. Antifungal activity of silver nanoparticles against Candida spp. *Biomaterials* **2009**, *30*, 6333–6340. [CrossRef] [PubMed]
18. Elgorban, A.M.; El-Samawaty, A.E.-R.M.; Yassin, M.A.; Sayed, S.R.; Adil, S.F.; Elhindi, K.M.; Bakri, M.; Khan, M. Antifungal silver nanoparticles: Synthesis, characterization and biological evaluation. *Biotechnol. Biotechnol. Equip.* **2015**, *30*, 56–62. [CrossRef]
19. Kanhed, P.; Birla, S.; Gaikwad, S.; Gade, A.; Seabra, A.B.; Rubilar, O.; Duran, N.; Rai, M. In vitro antifungal efficacy of copper nanoparticles against selected crop pathogenic fungi. *Mater. Lett.* **2014**, *115*, 13–17. [CrossRef]
20. Ponmurugan, P.; Manjukarunambika, K.; Elango, V.; Gnanamangai, B.M. Antifungal activity of biosynthesised copper nanoparticles evaluated against red root-rot disease in tea plants. *J. Exp. Nanosci.* **2016**, *11*, 1019–1031. [CrossRef]
21. Pariona, N.; Mtz-Enriquez, A.I.; Sánchez-Rangel, D.; Carrión, G.; Paraguay-Delgado, F.; Rosas-Saito, G. Green-synthesized copper nanoparticles as a potential antifungal against plant pathogens. *RSC Adv.* **2019**, *9*, 18835–18843. [CrossRef]
22. Paszkiewicz-Gawron, M.; Golabiewska, A.; Kowal, E.; Sajdak, A.; Zaleska-Medynska, A. Synthesis and Characterization of Monometallic (Ag, Cu) and Bimetallic Ag-Cu Particles for Antibacterial and Antifungal Applications. *J. Nanomater.* **2016**, *2016*, 1–11. [CrossRef]
23. Whitchurch, C.B.; Tolker-Nielsen, T.; Ragas, P.C.; Mattick, J.S. Extracellular DNA required for bacterial biofilm formation. *Science* **2002**, *295*, 1487. [CrossRef] [PubMed]
24. Fulaz, S.; Vitale, S.; Quinn, L.; Casey, E. Nanoparticle-Biofilm Interactions: The Role of the EPS Matrix. *Trends Microbiol.* **2019**, *27*, 915–926. [CrossRef]
25. Vu, B.; Chen, M.; Crawford, R.J.; Ivanova, E.P. Bacterial extracellular polysaccharides involved in biofilm formation. *Molecules* **2009**, *14*, 2535–2554. [CrossRef] [PubMed]
26. Jefferson, K.K. What drives bacteria to produce a biofilm? *FEMS Microbiol. Lett.* **2004**, *236*, 163–173. [CrossRef] [PubMed]
27. Sharma, D.; Misba, L.; Khan, A.U. Antibiotics versus biofilm: An emerging battleground in microbial communities. *Antimicrob. Resist. Infect. Control.* **2019**, *8*, 1–10. [CrossRef] [PubMed]
28. Liu, W.; Roder, H.L.; Madsen, J.S.; Bjarnsholt, T.; Sorensen, S.J.; Burmolle, M. Interspecific Bacterial Interactions are Reflected in Multispecies Biofilm Spatial Organization. *Front. Microbiol.* **2016**, *7*, 1366. [CrossRef] [PubMed]

29.　Rosenbaum, J.; Versace, D.L.; Abbad-Andallousi, S.; Pires, R.; Azevedo, C.; Cenedese, P.; Dubot, P. Antibacterial properties of nanostructured Cu-TiO2 surfaces for dental implants. *Biomater. Sci.* **2017**, *5*, 455–462. [CrossRef]

30.　McConoughey, S.J.; Howlin, R.; Granger, J.F.; Manring, M.M.; Calhoun, J.H.; Shirtliff, M.; Kathju, S.; Stoodley, P. Biofilms in periprosthetic orthopedic infections. *Future Microbiol.* **2014**, *9*, 987–1007. [CrossRef]

31.　Landini, P.; Antoniani, D.; Burgess, J.G.; Nijland, R. Molecular mechanisms of compounds affecting bacterial biofilm formation and dispersal. *Appl. Microbiol. Biotechnol.* **2010**, *86*, 813–823. [CrossRef] [PubMed]

32.　Vaidya, M.Y.; McBain, A.J.; Butler, J.A.; Banks, C.E.; Whitehead, K.A. Antimicrobial efficacy and synergy of metal ions against Enterococcus faecium, Klebsiella pneumoniae and Acinetobacter baumannii in planktonic and biofilm phenotypes. *Sci. Rep.* **2017**, *7*, 1–9. [CrossRef] [PubMed]

33.　Choi, O.; Yu, C.-P.; Fernández, G.E.; Hu, Z. Interactions of nanosilver with Escherichia coli cells in planktonic and biofilm cultures. *Water Res.* **2010**, *44*, 6095–6103. [CrossRef] [PubMed]

34.　Anderl, J.N.; Franklin, M.J.; Stewart, P.S. Role of antibiotic penetration limitation in Klebsiella pneumoniae biofilm resistance to ampicillin and ciprofloxacin. *Antimicrob. Agents Chemother.* **2000**, *44*, 1818–1824. [CrossRef]

35.　Emori, T.G.; Gaynes, R.P. An overview of nosocomial infections, including the role of the microbiology laboratory. *Clin. Microbiol. Rev.* **1993**, *6*, 428–442. [CrossRef] [PubMed]

36.　Edwardson, S.; Cairns, C. Nosocomial infections in the ICU. *Anaesth. Intensive Care Med.* **2019**, *20*, 14–18. [CrossRef]

37.　Kragh, K.N.; Hutchison, J.B.; Melaugh, G.; Rodesney, C.; Roberts, A.E.; Irie, Y.; Jensen, P.O.; Diggle, S.P.; Allen, R.J.; Gordon, V.; et al. Role of Multicellular Aggregates in Biofilm Formation. *mBio* **2016**, *7*, e00237. [CrossRef]

38.　Guillaume, O.; Perez-Tanoira, R.; Fortelny, R.; Redl, H.; Moriarty, T.F.; Richards, R.G.; Eglin, D.; Petter Puchner, A. Infections associated with mesh repairs of abdominal wall hernias: Are antimicrobial biomaterials the longed-for solution? *Biomaterials* **2018**, *167*, 15–31. [CrossRef]

39.　Chevalier, M.; Ranque, S.; Precheur, I. Oral fungal-bacterial biofilm models in vitro: A review. *Med. Mycol.* **2018**, *56*, 653–667. [CrossRef]

40.　James, G.A.; Boegli, L.; Hancock, J.; Bowersock, L.; Parker, A.; Kinney, B.M. Bacterial Adhesion and Biofilm Formation on Textured Breast Implant Shell Materials. *Aesthetic Plast. Surg.* **2019**, *43*, 490–497. [CrossRef]

41.　Filipović, U.; Dahmane, R.G.; Ghannouchi, S.; Zore, A.; Bohinc, K. Bacterial adhesion on orthopedic implants. *Adv. Colloid Interface Sci.* **2020**, *283*, 102228. [CrossRef]

42.　Ribeiro, M.; Monteiro, F.J.; Ferraz, M.P. Infection of orthopedic implants with emphasis on bacterial adhesion process and techniques used in studying bacterial-material interactions. *Biomatter* **2012**, *2*, 176–194. [CrossRef] [PubMed]

43.　Katsikogianni, M.; Missirlis, Y. Concise review of mechanisms of bacterial adhesion to biomaterials and of techniques used in estimating bacteria-material interactions. *Eur. Cell Mater.* **2004**, *8*, 37–57. [CrossRef] [PubMed]

44.　An, Y.H.; Friedman, R.J. Concise review of mechanisms of bacterial adhesion to biomaterial surfaces. *J. Biomed. Mater. Res.* **1998**, *43*, 338–348. [CrossRef]

45.　de Miguel, I.; Prieto, I.; Albornoz, A.; Sanz, V.; Weis, C.; Turon, P.; Quidant, R. Plasmon-Based Biofilm Inhibition on Surgical Implants. *Nano Lett.* **2019**, *19*, 2524–2529. [CrossRef]

46.　Kunrath, M.F.; Diz, F.M.; Magini, R.; Galárraga-Vinueza, M.E. Nanointeraction: The profound influence of nanostructured and nano-drug delivery biomedical implant surfaces on cell behavior. *Adv. Colloid Interface Sci.* **2020**, *284*, 102265. [CrossRef] [PubMed]

47.　Liao, J. Antibacterial titanium plate deposited by silver nanoparticles exhibits cell compatibility. *Int. J. Nanomed.* **2010**, *5*, 337–342.

48.　Juan, L. Deposition of silver nanoparticles on titanium surface for antibacterial effect. *Int. J. Nanomed.* **2010**, *5*, 261–267. [CrossRef] [PubMed]

49.　Li, S.; Liu, Y.; Tian, Z.; Liu, X.; Han, Z.; Ren, L. Biomimetic superhydrophobic and antibacterial stainless-steel mesh via double-potentiostatic electrodeposition and modification. *Surf. Coat. Technol.* **2020**, *403*, 126355. [CrossRef]

50.　Pashkuleva, I.; Marques, A.P.; Vaz, F.; Reis, R.L. Surface modification of starch based biomaterials by oxygen plasma or UV-irradiation. *J. Mater. Sci. Mater. Med.* **2010**, *21*, 21–32. [CrossRef]

51.　Li, X.; Qi, M.; Sun, X.; Weir, M.D.; Tay, F.R.; Oates, T.W.; Dong, B.; Zhou, Y.; Wang, L.; Xu, H.H. Surface treatments on titanium implants via nanostructured ceria for antibacterial and anti-inflammatory capabilities. *Acta Biomater.* **2019**, *94*, 627–643. [CrossRef]

52.　Dorobantu, L.S.; Fallone, C.; Noble, A.J.; Veinot, J.; Ma, G.; Goss, G.G.; Burrell, R.E. Toxicity of silver nanoparticles against bacteria, yeast, and algae. *J. Nanopart. Res.* **2015**, *17*. [CrossRef]

53.　Applerot, G.; Lipovsky, A.; Dror, R.; Perkas, N.; Nitzan, Y.; Lubart, R.; Gedanken, A. Enhanced Antibacterial Activity of Nanocrystalline ZnO Due to Increased ROS-Mediated Cell Injury. *Adv. Funct. Mater.* **2009**, *19*, 842–852. [CrossRef]

54.　Vincent, M.; Duval, R.E.; Hartemann, P.; Engels-Deutsch, M. Contact killing and antimicrobial properties of copper. *J. Appl. Microbiol.* **2018**, *124*, 1032–1046. [CrossRef]

55.　Tang, S.; Zheng, J. Antibacterial Activity of Silver Nanoparticles: Structural Effects. *Adv. Healthc. Mater.* **2018**, *7*, e1701503. [CrossRef] [PubMed]

56.　Crane, J.K. Metal Nanoparticles in Infection and Immunity. *Immunol. Investig.* **2020**, *49*, 794–807. [CrossRef] [PubMed]

57.　McQuillan, J.S.; Infante, H.G.; Stokes, E.; Shaw, A.M. Silver nanoparticle enhanced silver ion stress response in Escherichia coli K12. *Nanotoxicology* **2012**, *6*, 857–866. [CrossRef] [PubMed]

58. Bragg, P.; Rainnie, D. The effect of silver ions on the respiratory chain of Escherichia coli. *Can. J. Microbiol.* **1974**, *20*, 883–889. [CrossRef]

59. Panáček, A.; Kvitek, L.; Prucek, R.; Kolář, M.; Večeřová, R.; Pizúrová, N.; Sharma, V.K.; Nevěčná, T.j.; Zbořil, R. Silver colloid nanoparticles: Synthesis, characterization, and their antibacterial activity. *J. Phys. Chem. B* **2006**, *110*, 16248–16253. [CrossRef]

60. España-Sánchez, B.L.; Ávila-Orta, C.A.; Padilla-Vaca, F.; Neira-Velázquez, M.G.; González-Morones, P.; Rodríguez-González, J.A.; Hernández-Hernández, E.; Rangel-Serrano, Á.; Barriga-C, E.D.; Yate, L.; et al. Enhanced Antibacterial Activity of Melt Processed Poly(propylene) Ag and Cu Nanocomposites by Argon Plasma Treatment. *Plasma Process. Polym.* **2014**, *11*, 353–365. [CrossRef]

61. Xiu, Z.M.; Zhang, Q.B.; Puppala, H.L.; Colvin, V.L.; Alvarez, P.J. Negligible particle-specific antibacterial activity of silver nanoparticles. *Nano Lett.* **2012**, *12*, 4271–4275. [CrossRef]

62. Holt, K.B.; Bard, A.J. Interaction of silver (I) ions with the respiratory chain of Escherichia coli: An electrochemical and scanning electrochemical microscopy study of the antimicrobial mechanism of micromolar Ag+. *Biochemistry* **2005**, *44*, 13214–13223. [CrossRef] [PubMed]

63. Perez-Diaz, M.A.; Boegli, L.; James, G.; Velasquillo, C.; Sanchez-Sanchez, R.; Martinez-Martinez, R.E.; Martinez-Castanon, G.A.; Martinez-Gutierrez, F. Silver nanoparticles with antimicrobial activities against Streptococcus mutans and their cytotoxic effect. *Mater. Sci. Eng. C Mater. Biol Appl.* **2015**, *55*, 360–366. [CrossRef] [PubMed]

64. Lopez-Carballo, G.; Higueras, L.; Gavara, R.; Hernandez-Munoz, P. Silver ions release from antibacterial chitosan films containing in situ generated silver nanoparticles. *J. Agric. Food Chem.* **2013**, *61*, 260–267. [CrossRef]

65. El Badawy, A.; Silva, R.; Morris, B.; Scheckel, K.; Suidan, M.; Tolaymat, T. Surface charge-dependent toxicity of silver nanoparticles. *Environ. Sci. Technol.* **2011**, *45*, 283–287. [CrossRef]

66. van der Wal, A.; Norde, W.; Zehnder, A.J.; Lyklema, J. Determination of the total charge in the cell walls of Gram-positive bacteria. *Colloids Surf. B Biointerfaces* **1997**, *9*, 81–100. [CrossRef]

67. Harkes, G.; Van der Mei, H.; Rouxhet, P.; Dankert, J.; Busscher, H.; Feijen, J. Physicochemical characterization ofEscherichia coli. *Cell Biochem. Biophys.* **1992**, *20*, 17–32. [CrossRef] [PubMed]

68. Abbaszadegan, A.; Ghahramani, Y.; Gholami, A.; Hemmateenejad, B.; Dorostkar, S.; Nabavizadeh, M.; Sharghi, H. The Effect of Charge at the Surface of Silver Nanoparticles on Antimicrobial Activity against Gram-Positive and Gram-Negative Bacteria: A Preliminary Study. *J. Nanomater.* **2015**, *2015*, 1–8. [CrossRef]

69. Moloney, J.N.; Cotter, T.G. ROS signalling in the biology of cancer. *Semin. Cell Dev. Biol.* **2018**, *80*, 50–64. [CrossRef]

70. Zou, Z.; Chang, H.; Li, H.; Wang, S. Induction of reactive oxygen species: An emerging approach for cancer therapy. *Apoptosis* **2017**, *22*, 1321–1335. [CrossRef]

71. Park, M.V.; Neigh, A.M.; Vermeulen, J.P.; de la Fonteyne, L.J.; Verharen, H.W.; Briedé, J.J.; van Loveren, H.; de Jong, W.H. The effect of particle size on the cytotoxicity, inflammation, developmental toxicity and genotoxicity of silver nanoparticles. *Biomaterials* **2011**, *32*, 9810–9817. [CrossRef] [PubMed]

72. Cross, C.E.; Halliwell, B.; Borish, E.T.; Pryor, W.A.; Ames, B.N.; Saul, R.L.; McCord, J.M.; Harman, D. Oxygen radicals and human disease. *Ann. Intern. Med.* **1987**, *107*, 526–545. [CrossRef]

73. Dutta, R.K.; Nenavathu, B.P.; Gangishetty, M.K.; Reddy, A.V. Studies on antibacterial activity of ZnO nanoparticles by ROS induced lipid peroxidation. *Colloids Surf. B Biointerfaces* **2012**, *94*, 143–150. [CrossRef]

74. Choksi, K.B.; Boylston, W.H.; Rabek, J.P.; Widger, W.R.; Papaconstantinou, J. Oxidatively damaged proteins of heart mitochondrial electron transport complexes. *Biochim. Biophys. Acta* **2004**, *1688*, 95–101. [CrossRef] [PubMed]

75. Martinet, W.; De Meyer, G.; Herman, A.; Kockx, M. Reactive oxygen species induce RNA damage in human atherosclerosis. *Eur. J. Clin. Investig.* **2004**, *34*, 323–327. [CrossRef] [PubMed]

76. Dandona, P.; Thusu, K.; Cook, S.; Snyder, B.; Makowski, J.; Armstrong, D.; Nicotera, T. Oxidative damage to DNA in diabetes mellitus. *Lancet* **1996**, *347*, 444–445. [CrossRef]

77. Padmavathy, N.; Vijayaraghavan, R. Enhanced bioactivity of ZnO nanoparticles-an antimicrobial study. *Sci. Technol. Adv. Mater.* **2008**, *9*, 035004. [CrossRef] [PubMed]

78. Wang, L.; He, H.; Yu, Y.; Sun, L.; Liu, S.; Zhang, C.; He, L. Morphology-dependent bactericidal activities of Ag/CeO2 catalysts against Escherichia coli. *J. Inorg. Biochem.* **2014**, *100*, 45–53. [CrossRef]

79. Choi, O.; Hu, Z. Size dependent and reactive oxygen species related nanosilver toxicity to nitrifying bacteria. *Environ. Sci. Technol.* **2008**, *42*, 4583–4588. [CrossRef]

80. Wang, G.; Jin, W.; Qasim, A.M.; Gao, A.; Peng, X.; Li, W.; Feng, H.; Chu, P.K. Antibacterial effects of titanium embedded with silver nanoparticles based on electron-transfer-induced reactive oxygen species. *Biomaterials* **2017**, *124*, 25–34. [CrossRef]

81. Loran, S.; Cheng, S.; Botton, G.A.; Yahia, L.H.; Yelon, A.; Sacher, E. The physicochemical characterization of the Cu nanoparticle surface, and of its evolution on atmospheric exposure: Application to antimicrobial bandages for wound dressings. *Appl. Surf. Sci.* **2019**, *473*, 25–30. [CrossRef]

82. Grass, G.; Rensing, C.; Solioz, M. Metallic copper as an antimicrobial surface. *Appl. Environ. Microbiol.* **2011**, *77*, 1541–1547. [CrossRef] [PubMed]

83. Chillappagari, S.; Seubert, A.; Trip, H.; Kuipers, O.P.; Marahiel, M.A.; Miethke, M. Copper stress affects iron homeostasis by destabilizing iron-sulfur cluster formation in Bacillus subtilis. *J. Bacteriol.* **2010**, *192*, 2512–2524. [CrossRef] [PubMed]

84. Rtimi, S.; Dionysiou, D.D.; Pillai, S.C.; Kiwi, J. Advances in catalytic/photocatalytic bacterial inactivation by nano Ag and Cu coated surfaces and medical devices. *Appl. Catal. B Environ.* **2019**, *240*, 291–318. [CrossRef]

85. Macomber, L.; Rensing, C.; Imlay, J.A. Intracellular copper does not catalyze the formation of oxidative DNA damage in Escherichia coli. *J. Bacteriol.* **2007**, *189*, 1616–1626. [CrossRef]

86. Loran, S.; Yelon, A.; Sacher, E. Short communication: Unexpected findings on the physicochemical characterization of the silver nanoparticle surface. *Appl. Surf. Sci.* **2018**, *428*, 1079–1081. [CrossRef]

87. Duran, N.; Duran, M.; de Jesus, M.B.; Seabra, A.B.; Favaro, W.J.; Nakazato, G. Silver nanoparticles: A new view on mechanistic aspects on antimicrobial activity. *Nanomedicine* **2016**, *12*, 789–799. [CrossRef]

88. Li, Y.; Dong, Y.; Yang, Y.; Yu, P.; Zhang, Y.; Hu, J.; Li, T.; Zhang, X.; Liu, X.; Xu, Q. Rational design of silver gradient for studying size effect of silver nanoparticles on contact killing. *ACS Biomater. Sci. Eng.* **2018**, *5*, 425–431. [CrossRef]

89. Agnihotri, S.; Mukherji, S.; Mukherji, S. Immobilized silver nanoparticles enhance contact killing and show highest efficacy: Elucidation of the mechanism of bactericidal action of silver. *Nanoscale* **2013**, *5*, 7328–7340. [CrossRef]

90. Zawadzka, K.; Kisielewska, A.; Piwoński, I.; Kądzioła, K.; Felczak, A.; Różalska, S.; Wrońska, N.; Lisowska, K. Mechanisms of antibacterial activity and stability of silver nanoparticles grown on magnetron sputtered TiO 2 coatings. *Bull. Mater. Sci.* **2016**, *39*, 57–68. [CrossRef]

91. Reidy, B.; Haase, A.; Luch, A.; Dawson, K.A.; Lynch, I. Mechanisms of Silver Nanoparticle Release, Transformation and Toxicity: A Critical Review of Current Knowledge and Recommendations for Future Studies and Applications. *Materials* **2013**, *6*, 2295–2350. [CrossRef]

92. Yin, I.X.; Zhang, J.; Zhao, I.S.; Mei, M.L.; Li, Q.; Chu, C.H. The Antibacterial Mechanism of Silver Nanoparticles and Its Application in Dentistry. *Int. J. Nanomed.* **2020**, *15*, 2555. [CrossRef]

93. Yan, X.; He, B.; Liu, L.; Qu, G.; Shi, J.; Hu, L.; Jiang, G. Antibacterial mechanism of silver nanoparticles in Pseudomonas aeruginosa: Proteomics approach. *Metallomics* **2018**, *10*, 557–564. [CrossRef]

94. Fang, F.C. Antimicrobial reactive oxygen and nitrogen species: Concepts and controversies. *Nat. Rev. Microbiol.* **2004**, *2*, 820–832. [CrossRef] [PubMed]

95. Pant, J.; Goudie, M.J.; Hopkins, S.P.; Brisbois, E.J.; Handa, H. Tunable nitric oxide release from S-nitroso-N-acetylpenicillamine via catalytic copper nanoparticles for biomedical applications. *ACS Appl. Mater. Interfaces* **2017**, *9*, 15254–15264. [CrossRef] [PubMed]

96. Rolim, W.R.; Pieretti, J.C.; Renó, D.b.L.; Lima, B.A.; Nascimento, M.N.H.; Ambrosio, F.N.; Lombello, C.B.; Brocchi, M.; de Souza, A.C.S.; Seabra, A.B. Antimicrobial activity and cytotoxicity to tumor cells of nitric oxide donor and silver nanoparticles containing PVA/PEG films for topical applications. *ACS Appl. Mater. Interfaces* **2019**, *11*, 6589–6604. [CrossRef]

97. Ganz, T. Defensins: Antimicrobial peptides of innate immunity. *Nat. Rev. Immunol.* **2003**, *3*, 710–720. [CrossRef]

98. Biswaro, L.S.; da Costa Sousa, M.G.; Rezende, T.M.B.; Dias, S.C.; Franco, O.L. Antimicrobial Peptides and Nanotechnology, Recent Advances and Challenges. *Front. Microbiol.* **2018**, *9*. [CrossRef]

99. Ruden, S.; Hilpert, K.; Berditsch, M.; Wadhwani, P.; Ulrich, A.S. Synergistic interaction between silver nanoparticles and membrane-permeabilizing antimicrobial peptides. *Antimicrob. Agents Chemother.* **2009**, *53*, 3538–3540. [CrossRef]

100. Sun, B.; Xia, T. Nanomaterial-based vaccine adjuvants. *J. Mater. Chem. B* **2016**, *4*, 5496–5509. [CrossRef] [PubMed]

101. Xu, Y.; Tang, H.; Liu, J.-h.; Wang, H.; Liu, Y. Evaluation of the adjuvant effect of silver nanoparticles both in vitro and in vivo. *Toxicol. Lett.* **2013**, *219*, 42–48. [CrossRef]

102. Poggio, C.; Colombo, M.; Arciola, C.R.; Greggi, T.; Scribante, A.; Dagna, A. Copper-Alloy Surfaces and Cleaning Regimens against the Spread of SARS-CoV-2 in Dentistry and Orthopedics. From Fomites to Anti-Infective Nanocoatings. *Materials* **2020**, *13*, 3244. [CrossRef] [PubMed]

103. Zhou, J.; Hu, Z.; Zabihi, F.; Chen, Z.; Zhu, M. Progress and Perspective of Antiviral Protective Material. *Adv. Fiber Mater.* **2020**, *2*, 123–139. [CrossRef]

104. Weiss, C.; Carriere, M.; Fusco, L.; Capua, I.; Regla-Nava, J.A.; Pasquali, M.; Scott, J.A.; Vitale, F.; Unal, M.A.; Mattevi, C.; et al. Toward Nanotechnology-Enabled Approaches against the COVID-19 Pandemic. *ACS Nano* **2020**, *14*, 6383–6406. [CrossRef]

105. Thi Ngoc Dung, T.; Nang Nam, V.; Thi Nhan, T.; Ngoc, T.T.B.; Minh, L.Q.; Nga, B.T.T.; Phan Le, V.; Viet Quang, D. Silver nanoparticles as potential antiviral agents against African swine fever virus. *Mater. Res. Express* **2020**, *6*. [CrossRef]

106. Du, T.; Liang, J.; Dong, N.; Lu, J.; Fu, Y.; Fang, L.; Xiao, S.; Han, H. Glutathione-Capped Ag2S Nanoclusters Inhibit Coronavirus Proliferation through Blockage of Viral RNA Synthesis and Budding. *ACS Appl. Mater. Interfaces* **2018**, *10*, 4369–4378. [CrossRef]

107. Rai, M.; Deshmukh, S.D.; Ingle, A.P.; Gupta, I.R.; Galdiero, M.; Galdiero, S. Metal nanoparticles: The protective nanoshield against virus infection. *Crit. Rev. Microbiol.* **2016**, *42*, 46–56. [CrossRef]

108. Warnes, S.L.; Summersgill, E.N.; Keevil, C.W. Inactivation of murine norovirus on a range of copper alloy surfaces is accompanied by loss of capsid integrity. *Appl. Environ. Microbiol.* **2015**, *81*, 1085–1091. [CrossRef] [PubMed]

109. Tavakoli, A.; Hashemzadeh, M.S. Inhibition of herpes simplex virus type 1 by copper oxide nanoparticles. *J. Virol. Methods* **2020**, *275*, 113688. [CrossRef]

110. Slavin, Y.N.; Asnis, J.; Hafeli, U.O.; Bach, H. Metal nanoparticles: Understanding the mechanisms behind antibacterial activity. *J. Nanobiotechnol.* **2017**, *15*, 65. [CrossRef] [PubMed]

111. Tamayo, L.A.; Zapata, P.A.; Vejar, N.D.; Azocar, M.I.; Gulppi, M.A.; Zhou, X.; Thompson, G.E.; Rabagliati, F.M.; Paez, M.A. Release of silver and copper nanoparticles from polyethylene nanocomposites and their penetration into Listeria monocytogenes. *Mater. Sci. Eng. C Mater. Biol. Appl.* **2014**, *40*, 24–31. [CrossRef] [PubMed]

112. Rather, R.A.; Sarwara, R.K.; Das, N.; Pal, B. Impact of reducing and capping agents on carbohydrates for the growth of Ag and Cu nanostructures and their antibacterial activities. *Particuology* **2019**, *43*, 219–226. [CrossRef]

113. Mukherji, S.; Ruparelia, J.; Agnihotri, S. Antimicrobial activity of silver and copper nanoparticles: Variation in sensitivity across various strains of bacteria and fungi. In *Nano-Antimicrobials Progress and Prospects*; Cioffi, N., Rai, M., Eds.; Springer: Heidelberg, Germany, 2012; pp. 225–251.

114. Fellahi, O.; Sarma, R.K.; Das, M.R.; Saikia, R.; Marcon, L.; Coffinier, Y.; Hadjersi, T.; Maamache, M.; Boukherroub, R. The antimicrobial effect of silicon nanowires decorated with silver and copper nanoparticles. *Nanotechnology* **2013**, *24*, 495101. [CrossRef]

115. Ruparelia, J.P.; Chatterjee, A.K.; Duttagupta, S.P.; Mukherji, S. Strain specificity in antimicrobial activity of silver and copper nanoparticles. *Acta Biomater.* **2008**, *4*, 707–716. [CrossRef]

116. Rtimi, S.; Sanjines, R.; Pulgarin, C.; Kiwi, J. Microstructure of Cu-Ag Uniform Nanoparticulate Films on Polyurethane 3D Catheters: Surface Properties. *ACS Appl. Mater. Interfaces* **2016**, *8*, 56–63. [CrossRef] [PubMed]

117. Ivask, A.; ElBadawy, A.; Kaweeteerawat, C.; Boren, D.; Fischer, H.; Ji, Z.; Chang, C.H.; Liu, R.; Tolaymat, T.; Telesca, D. Toxicity mechanisms in Escherichia coli vary for silver nanoparticles and differ from ionic silver. *ACS Nano* **2014**, *8*, 374–386. [CrossRef]

118. Asghar, M.A.; Zahir, E.; Shahid, S.M.; Khan, M.N.; Asghar, M.A.; Iqbal, J.; Walker, G. Iron, copper and silver nanoparticles: Green synthesis using green and black tea leaves extracts and evaluation of antibacterial, antifungal and aflatoxin B1 adsorption activity. *LWT* **2018**, *90*, 98–107. [CrossRef]

119. Gunputh, U.F.; Le, H.; Handy, R.D.; Tredwin, C. Anodised TiO2 nanotubes as a scaffold for antibacterial silver nanoparticles on titanium implants. *Mater. Sci. Eng. C* **2018**, *100*, 638–644. [CrossRef]

120. Singh, S.; Bharti, A.; Meena, V.K. Green synthesis of multi-shaped silver nanoparticles: Optical, morphological and antibacterial properties. *J. Mater. Sci. Mater. Electron.* **2015**, *26*, 3638–3648. [CrossRef]

121. Pal, S.; Tak, Y.K.; Song, J.M. Does the antibacterial activity of silver nanoparticles depend on the shape of the nanoparticle? A study of the gram-negative bacterium Escherichia coli. *Appl. Environ. Microbiol.* **2007**, *73*, 1712–1720. [CrossRef]

122. El-Zahry, M.R.; Mahmoud, A.; Refaat, I.H.; Mohamed, H.A.; Bohlmann, H.; Lendl, B. Antibacterial effect of various shapes of silver nanoparticles monitored by SERS. *Talanta* **2015**, *138*, 183–189. [CrossRef] [PubMed]

123. Vankayala, R.; Kuo, C.-L.; Sagadevan, A.; Chen, P.-H.; Chiang, C.-S.; Hwang, K.C. Morphology dependent photosensitization and formation of singlet oxygen (1 Δ g) by gold and silver nanoparticles and its application in cancer treatment. *J. Mater. Chem. B* **2013**, *1*, 4379–4387. [CrossRef]

124. Maniprasad, P.; Menezes, R.; Suarez, J.; Santra, S. Antimicrobial properties of copper and silver loaded silica nanomaterials. In *Nanostructured Materials and Nanotechnology VI*; Mathur, S., Ray, S.S., Eds.; Springer: Hoboken, NJ, USA, 2012; pp. 55–67.

125. Kvítek, L.; Panáček, A.; Soukupova, J.; Kolář, M.; Večeřová, R.; Prucek, R.; Holecova, M.; Zbořil, R. Effect of surfactants and polymers on stability and antibacterial activity of silver nanoparticles (NPs). *J. Phys. Chem. C* **2008**, *112*, 5825–5834. [CrossRef]

126. Valodkar, M.; Modi, S.; Pal, A.; Thakore, S. Synthesis and anti-bacterial activity of Cu, Ag and Cu–Ag alloy nanoparticles: A green approach. *Mater. Res. Bull.* **2011**, *46*, 384–389. [CrossRef]

127. Mohan, R.; Shanmugharaj, A.M.; Sung Hun, R. An efficient growth of silver and copper nanoparticles on multiwalled carbon nanotube with enhanced antimicrobial activity. *J. Biomed. Mater. Res. B Appl. Biomater.* **2011**, *96*, 119–126. [CrossRef] [PubMed]

128. Hemeg, H.A. Nanomaterials for alternative antibacterial therapy. *Int. J. Nanomed.* **2017**, *12*, 8211–8225. [CrossRef]

129. Naqvi, S.; Kiran, U.; Ali, M.; Jamal, A.; Hameed, A.; Ahmed, S.; Ali, N. Combined efficacy of biologically synthesized silver nanoparticles and different antibiotics against multidrug-resistant bacteria. *Int. J. Nanomed.* **2013**, *8*, 3187–3195. [CrossRef]

130. Kiranmai, M.; Kadimcharla, K.; Keesara, N.R.; Fatima, S.N.; Bommena, P.; Batchu, U.R. Green synthesis of stable copper nanoparticles and synergistic activity with antibiotics. *Indian J. Pharm. Sci.* **2017**, *79*, 695–700.

131. Panáček, A.; Smékalová, M.; Kilianová, M.; Prucek, R.; Bogdanová, K.; Večeřová, R.; Kolář, M.; Havrdová, M.; Płaza, G.A.; Chojniak, J. Strong and nonspecific synergistic antibacterial efficiency of antibiotics combined with silver nanoparticles at very low concentrations showing no cytotoxic effect. *Molecules* **2016**, *21*, 26. [CrossRef]

132. Hu, Z.; Chan, W.L.; Szeto, Y.S. Nanocomposite of chitosan and silver oxide and its antibacterial property. *J. Appl. Polym. Sci.* **2008**, *108*, 52–56. [CrossRef]

133. Mahlaule-Glory, L.; Mbita, Z.; Mathipa, M.; Tetana, Z.; Hintsho-Mbita, N. Biological therapeutics of AgO nanoparticles against pathogenic bacteria and A549 lung cancer cells. *Mater. Res. Express* **2019**, *6*, 105402. [CrossRef]

134. Haq, S.; Rehman, W.; Waseem, M.; Meynen, V.; Awan, S.U.; Saeed, S.; Iqbal, N. Fabrication of pure and moxifloxacin functionalized silver oxide nanoparticles for photocatalytic and antimicrobial activity. *J. Photochem. Photobiol. B Biol.* **2018**, *186*, 116–124. [CrossRef]

135. Applerot, G.; Lellouche, J.; Lipovsky, A.; Nitzan, Y.; Lubart, R.; Gedanken, A.; Banin, E. Understanding the antibacterial mechanism of CuO nanoparticles: Revealing the route of induced oxidative stress. *Small* **2012**, *8*, 3326–3337. [CrossRef] [PubMed]

136. Meghana, S.; Kabra, P.; Chakraborty, S.; Padmavathy, N. Understanding the pathway of antibacterial activity of copper oxide nanoparticles. *RSC Adv.* **2015**, *5*, 12293–12299. [CrossRef]

137. Ren, G.; Hu, D.; Cheng, E.W.; Vargas-Reus, M.A.; Reip, P.; Allaker, R.P. Characterisation of copper oxide nanoparticles for antimicrobial applications. *Int. J. Antimicrob. Agents* **2009**, *33*, 587–590. [CrossRef]

138. Das, D.; Nath, B.C.; Phukon, P.; Dolui, S.K. Synthesis and evaluation of antioxidant and antibacterial behavior of CuO nanoparticles. *Colloids Surf. B Biointerfaces* **2013**, *101*, 430–433. [CrossRef] [PubMed]

139. Kumar, D.A.; Palanichamy, V.; Roopan, S.M. Photocatalytic action of AgCl nanoparticles and its antibacterial activity. *J. Photochem. Photobiol. B Biol.* **2014**, *138*, 302–306. [CrossRef] [PubMed]

140. Wang, X.; Sui, Y.; Jian, J.; Yuan, Z.; Zeng, J.; Zhang, L.; Wang, T.; Zhou, H. Ag@ AgCl nanoparticles in-situ deposited cellulose acetate/silk fibroin composite film for photocatalytic and antibacterial applications. *Cellulose* **2020**, *27*, 7721–7737. [CrossRef]

141. Dong, L.; Liang, D.; Gong, R. In Situ Photoactivated AgCl/Ag Nanocomposites with Enhanced Visible Light Photocatalytic and Antibacterial Activity. *Eur. J. Inorg. Chem.* **2012**, *2012*, 3200–3208. [CrossRef]

142. Liu, Z.; Guo, W.; Guo, C.; Liu, S. Fabrication of AgBr nanomaterials as excellent antibacterial agents. *RSC Adv.* **2015**, *5*, 72872–72880. [CrossRef]

143. Rehan, M.; Khattab, T.A.; Barohum, A.; Gatjen, L.; Wilken, R. Development of Ag/AgX (X=Cl, I) nanoparticles toward antimicrobial, UV-protected and self-cleanable viscose fibers. *Carbohydr. Polym.* **2018**, *197*, 227–236. [CrossRef]

144. Tan, P.; Li, Y.-H.; Liu, X.-Q.; Jiang, Y.; Sun, L.-B. Core–Shell AgCl@SiO2 Nanoparticles: Ag(I)-Based Antibacterial Materials with Enhanced Stability. *ACS Sustain. Chem. Eng.* **2016**, *4*, 3268–3275. [CrossRef]

145. Subramaniyan, S.B.; Megarajan, S.; Vijayakumar, S.; Mariappan, M.; Anbazhagan, V. Evaluation of the toxicities of silver and silver sulfide nanoparticles against Gram-positive and Gram-negative bacteria. *IET Nanobiotechnol.* **2018**, *13*, 326–331. [CrossRef]

146. Delgado-Beleño, Y.; Martinez-Nuñez, C.E.; Cortez-Valadez, M.; Flores-López, N.S.; Flores-Acosta, M. Optical properties of silver, silver sulfide and silver selenide nanoparticles and antibacterial applications. *Mater. Res. Bull.* **2018**, *99*, 385–392. [CrossRef]

147. Shalabayev, Z.; Baláž, M.; Daneu, N.; Dutková, E.; Bujňáková, Z.; Kaňuchová, M.; Danková, Z.; Balážová, Ľ.; Urakaev, F.; Tkáčiková, Ľ.; et al. Sulfur-Mediated Mechanochemical Synthesis of Spherical and Needle-Like Copper Sulfide Nanocrystals with Antibacterial Activity. *ACS Sustain. Chem. Eng.* **2019**, *7*, 12897–12909. [CrossRef]

148. Huang, J.; Zhou, J.; Zhuang, J.; Gao, H.; Huang, D.; Wang, L.; Wu, W.; Li, Q.; Yang, D.P.; Han, M.Y. Strong Near-Infrared Absorbing and Biocompatible CuS Nanoparticles for Rapid and Efficient Photothermal Ablation of Gram-Positive and -Negative Bacteria. *ACS Appl. Mater. Interfaces* **2017**, *9*, 36606–36614. [CrossRef]

149. Qiao, Y.; Ping, Y.; Zhang, H.; Zhou, B.; Liu, F.; Yu, Y.; Xie, T.; Li, W.; Zhong, D.; Zhang, Y.; et al. Laser-Activatable CuS Nanodots to Treat Multidrug-Resistant Bacteria and Release Copper Ion to Accelerate Healing of Infected Chronic Nonhealing Wounds. *ACS Appl. Mater. Interfaces* **2019**, *11*, 3809–3822. [CrossRef] [PubMed]

150. Wang, H.Y.; Hua, X.W.; Wu, F.G.; Li, B.; Liu, P.; Gu, N.; Wang, Z.; Chen, Z. Synthesis of ultrastable copper sulfide nanoclusters via trapping the reaction intermediate: Potential anticancer and antibacterial applications. *ACS Appl. Mater. Interfaces* **2015**, *7*, 7082–7092. [CrossRef] [PubMed]

151. Chen, H.; Wang, B.; Zhang, J.; Nie, C.; Lv, F.; Liu, L.; Wang, S. Guanidinium-pendant oligofluorene for rapid and specific identification of antibiotics with membrane-disrupting ability. *Chem. Commun.* **2015**, *51*, 4036–4039. [CrossRef] [PubMed]

152. Chen, K.-T.; Ray, D.; Peng, Y.-H.; Hsu, Y.-C. Preparation of Cu–Ag core–shell particles with their anti-oxidation and antibacterial properties. *Curr. Appl. Phys.* **2013**, *13*, 1496–1501. [CrossRef]

153. Yoon, K.Y.; Hoon Byeon, J.; Park, J.H.; Hwang, J. Susceptibility constants of Escherichia coli and Bacillus subtilis to silver and copper nanoparticles. *Sci. Total Environ.* **2007**, *373*, 572–575. [CrossRef]

154. Phan, D.-N.; Dorjjugder, N.; Khan, M.Q.; Saito, Y.; Taguchi, G.; Lee, H.; Mukai, Y.; Kim, I.-S. Synthesis and attachment of silver and copper nanoparticles on cellulose nanofibers and comparative antibacterial study. *Cellulose* **2019**, *26*, 6629–6640. [CrossRef]

155. Muller, M. Bacterial Silver Resistance Gained by Cooperative Interspecies Redox Behavior. *Antimicrob. Agents Chemother.* **2018**, *62*, e00672-00618. [CrossRef]

156. Feßler, A.T.; Zhao, Q.; Schoenfelder, S.; Kadlec, K.; Michael, G.B.; Wang, Y.; Ziebuhr, W.; Shen, J.; Schwarz, S. Complete sequence of a plasmid from a bovine methicillin-resistant Staphylococcus aureus harbouring a novel ica-like gene cluster in addition to antimicrobial and heavy metal resistance genes. *Vet. Microbiol.* **2017**, *100*, 95–100. [CrossRef] [PubMed]

157. Purves, J.; Thomas, J.; Riboldi, G.P.; Zapotoczna, M.; Tarrant, E.; Andrew, P.W.; Londoño, A.; Planet, P.J.; Geoghegan, J.A.; Waldron, K.J. A horizontally gene transferred copper resistance locus confers hyper-resistance to antibacterial copper toxicity and enables survival of community acquired methicillin resistant Staphylococcus aureus USA300 in macrophages. *Environ. Microbiol.* **2018**, *20*, 1576–1589. [CrossRef]

158. Kunito, T.; Saeki, K.; Nagaoka, K.; Oyaizu, H.; Matsumoto, S. Characterization of copper-resistant bacterial community in rhizosphere of highly copper-contaminated soil. *Eur. J. Soil Biol.* **2001**, *37*, 95–102. [CrossRef]

159. Altimira, F.; Yáñez, C.; Bravo, G.; González, M.; Rojas, L.A.; Seeger, M. Characterization of copper-resistant bacteria and bacterial communities from copper-polluted agricultural soils of central Chile. *BMC Microbiol.* **2012**, *12*, 1–12. [CrossRef]

160. Torres-Urquidy, O.; Bright, K. Efficacy of multiple metals against copper-resistant bacterial strains. *J. Appl. Microbiol.* **2012**, *112*, 695–704. [CrossRef] [PubMed]

161. Silver, S. Bacterial silver resistance: Molecular biology and uses and misuses of silver compounds. *FEMS Microbiol. Rev.* **2003**, *27*, 341–353. [CrossRef]

162. Li, X.Z.; Nikaido, H.; Williams, K.E. Silver-resistant mutants of Escherichia coli display active efflux of Ag+ and are deficient in porins. *J. Bacteriol.* **1997**, *179*, 6127–6132. [CrossRef] [PubMed]

163. Prabhu, S.; Poulose, E.K. Silver nanoparticles: Mechanism of antimicrobial action, synthesis, medical applications, and toxicity effects. *Int. Nano Lett.* **2012**, *2*, 1–10. [CrossRef]

164. Cortizo, M.C.; De Mele, M.F.L. Cytotoxicity of copper ions released from metal. *Biol. Trace Elem. Res.* **2004**, *102*, 129–141. [CrossRef]

165. Vimbela, G.; Ngo, S.; Fraze, C.; Yang, L.; Stout, D. Antibacterial properties and toxicity from metallic nanomaterials. *Int. J. Nanomed.* **2017**, *12*, 3941–3965. [CrossRef]

166. Nel, A.; Xia, T.; Mädler, L.; Li, N. Toxic potential of materials at the nanolevel. *Science* **2006**, *311*, 622–627. [CrossRef]

167. Bartlomiejczyk, T.; Lankoff, A.; Kruszewski, M.; Szumiel, I. Silver nanoparticles–allies or adversaries? *Ann. Agric. Environ. Med.* **2013**, *20*, 48–54. [PubMed]

168. Martínez-Gutierrez, F.; Thi, E.P.; Silverman, J.M.; de Oliveira, C.C.; Svensson, S.L.; Hoek, A.V.; Sánchez, E.M.; Reiner, N.E.; Gaynor, E.C.; Pryzdial, E.L. Antibacterial activity, inflammatory response, coagulation and cytotoxicity effects of silver nanoparticles. *Nanomed. Nanotechnol. Biol. Med.* **2012**, *8*, 328–336. [CrossRef]

169. Ingle, A.P.; Duran, N.; Rai, M. Bioactivity, mechanism of action, and cytotoxicity of copper-based nanoparticles: A review. *Appl. Microbiol. Biotechnol.* **2014**, *98*, 1001–1009. [CrossRef]

170. Ballo, M.K.; Rtimi, S.; Pulgarin, C.; Hopf, N.; Berthet, A.; Kiwi, J.; Moreillon, P.; Entenza, J.M.; Bizzini, A. In vitro and in vivo effectiveness of an innovative silver-copper nanoparticle coating of catheters to prevent methicillin-resistant Staphylococcus aureus infection. *Antimicrob. Agents Chemother.* **2016**, *60*, 5349–5356. [CrossRef] [PubMed]

171. Sowa-Söhle, E.N.; Schwenke, A.; Wagener, P.; Weiss, A.; Wiegel, H.; Sajti, C.L.; Haverich, A.; Barcikowski, S.; Loos, A. Antimicrobial efficacy, cytotoxicity, and ion release of mixed metal (Ag, Cu, Zn, Mg) nanoparticle polymer composite implant material. *BioNanoMaterials* **2013**, *14*, 217–227. [CrossRef]

172. Hackenberg, S.; Scherzed, A.; Kessler, M.; Hummel, S.; Technau, A.; Froelich, K.; Ginzkey, C.; Koehler, C.; Hagen, R.; Kleinsasser, N. Silver nanoparticles: Evaluation of DNA damage, toxicity and functional impairment in human mesenchymal stem cells. *Toxicol. Lett.* **2011**, *201*, 27–33. [CrossRef]

173. Kim, Y.S.; Kim, K.K.; Shin, S.; Park, S.M.; Hah, S.S. Comparative toxicity studies of ultra-pure Ag, Au, Co, and Cu nanoparticles generated by laser ablation in biocompatible aqueous solution. *Bull. Korean Chem. Soc.* **2012**, *33*, 3265–3268. [CrossRef]

174. Chen, Y.-N.; Hsueh, Y.-H.; Hsieh, C.-T.; Tzou, D.-Y.; Chang, P.-L. Antiviral activity of graphene–silver nanocomposites against non-enveloped and enveloped viruses. *Int. J. Environ. Res. Public Health* **2016**, *13*, 430. [CrossRef]

175. Xie, C.M.; Lu, X.; Wang, K.F.; Meng, F.Z.; Jiang, O.; Zhang, H.P.; Zhi, W.; Fang, L.M. Silver nanoparticles and growth factors incorporated hydroxyapatite coatings on metallic implant surfaces for enhancement of osteoinductivity and antibacterial properties. *ACS Appl. Mater. Interfaces* **2014**, *6*, 8580–8589. [CrossRef] [PubMed]

176. Park, J.; Ham, S.; Jang, M.; Lee, J.; Kim, S.; Kim, S.; Lee, K.; Park, D.; Kwon, J.; Kim, H.; et al. Spatial-Temporal Dispersion of Aerosolized Nanoparticles During the Use of Consumer Spray Products and Estimates of Inhalation Exposure. *Environ. Sci. Technol.* **2017**, *51*, 7624–7638. [CrossRef] [PubMed]

177. Kim, E.; Lee, J.H.; Kim, J.K.; Lee, G.H.; Ahn, K.; Park, J.D.; Yu, I.J. Case study on risk evaluation of silver nanoparticle exposure from antibacterial sprays containing silver nanoparticles. *J. Nanomater.* **2015**, *2015*, 8. [CrossRef]

178. Ahmed, J.; Mulla, M.; Arfat, Y.A.; Bher, A.; Jacob, H.; Auras, R. Compression molded LLDPE films loaded with bimetallic (Ag-Cu) nanoparticles and cinnamon essential oil for chicken meat packaging applications. *LWT* **2018**, *93*, 329–338. [CrossRef]

179. Picca, R.A.; Di Maria, A.; Riháková, L.; Volpe, A.; Sportelli, M.C.; Lugarà, P.M.; Ancona, A.; Cioffi, N. Laser ablation synthesis of hybrid copper/silver Nanocolloids for prospective application as Nanoantimicrobial agents for food packaging. *MRS Adv.* **2016**, *1*, 3735–3740. [CrossRef]

180. Dankovich, T.A.; Smith, J.A. Incorporation of copper nanoparticles into paper for point-of-use water purification. *Water Res.* **2014**, *63*, 245–251. [CrossRef] [PubMed]

181. Yakub, I.; Soboyejo, W. Adhesion of E. coli to silver-or copper-coated porous clay ceramic surfaces. *J. Appl. Phys.* **2012**, *111*, 124324. [CrossRef]

182. Joe, Y.H.; Ju, W.; Park, J.H.; Yoon, Y.H.; Hwang, J. Correlation between the antibacterial ability of silver nanoparticle coated air filters and the dust loading. *Aerosol Air Qual. Res.* **2013**, *13*, 1009–1018. [CrossRef]

183. Le, T.S.; Dao, T.H.; Nguyen, D.C.; Nguyen, H.C.; Balikhin, I. Air purification equipment combining a filter coated by silver nanoparticles with a nano-TiO2 photocatalyst for use in hospitals. *Adv. Nat. Sci. Nanosci. Nanotechnol.* **2015**, *6*, 015016. [CrossRef]

184. Chiome, T.; Srinivasan, A. Use of antiviral nanocoating in personal protective wear. *Int. J. Health Allied Sci.* **2020**, *9*, 62–67. [CrossRef]

185. Borkow, G.; Zhou, S.S.; Page, T.; Gabbay, J. A novel anti-influenza copper oxide containing respiratory face mask. *PLoS ONE* **2010**, *5*, e11295. [CrossRef] [PubMed]

186. Borkow, G.; Gabbay, J. Biocidal textiles can help fight nosocomial infections. *Med. Hypotheses* **2008**, *70*, 990–994. [CrossRef] [PubMed]

187. Wang, K.; Ma, Q.; Zhang, Y.; Wang, S.; Han, G. Ag NPs-Assisted Synthesis of Stable Cu NPs on PET Fabrics for Antibacterial and Electromagnetic Shielding Performance. *Polymers* **2020**, *12*, 783. [CrossRef] [PubMed]

188. Eremenko, A.M.; Petrik, I.S.; Smirnova, N.P.; Rudenko, A.V.; Marikvas, Y.S. Antibacterial and Antimycotic Activity of Cotton Fabrics, Impregnated with Silver and Binary Silver/Copper Nanoparticles. *Nanoscale Res. Lett.* **2016**, *11*, 28. [CrossRef] [PubMed]

189. Lorenz, C.; Windler, L.; von Goetz, N.; Lehmann, R.; Schuppler, M.; Hungerbühler, K.; Heuberger, M.; Nowack, B. Characterization of silver release from commercially available functional (nano) textiles. *Chemosphere* **2012**, *89*, 817–824. [CrossRef] [PubMed]

190. Paszkiewicz, M.; Gołąbiewska, A.; Rajski, Ł.; Kowal, E.; Sajdak, A.; Zaleska-Medynska, A. The Antibacterial and Antifungal Textile Properties Functionalized by Bimetallic Nanoparticles of Ag/Cu with Different Structures. *J. Nanomater.* **2016**, *2016*, 1–13. [CrossRef]

191. Shahidi, S.; Moazzenchi, B. The Influence of Dyeing on the Adsorption of Silver and Copper Particles as Antibacterial Agents on to Cotton Fabrics. *J. Nat. Fibers* **2018**, *16*, 677–687. [CrossRef]

192. Hassabo, A.G.; El-Naggar, M.E.; Mohamed, A.L.; Hebeish, A.A. Development of multifunctional modified cotton fabric with tri-component nanoparticles of silver, copper and zinc oxide. *Carbohydr. Polym.* **2019**, *210*, 144–156. [CrossRef]

193. Harrasser, N.; Jüssen, S.; Obermeir, A.; Kmeth, R.; Stritzker, B.; Gollwitzer, H.; Burgkart, R. Antibacterial potency of different deposition methods of silver and copper containing diamond-like carbon coated polyethylene. *Biomater. Res.* **2016**, *20*, 1–10. [CrossRef] [PubMed]

194. Stelzig, S.H.; Menneking, C.; Hoffmann, M.S.; Eisele, K.; Barcikowski, S.; Klapper, M.; Müllen, K. Compatibilization of laser generated antibacterial Ag-and Cu-nanoparticles for perfluorinated implant materials. *Eur. Polym. J.* **2011**, *47*, 662–667. [CrossRef]

195. Hench, L.L. Bioceramics: From concept to clinic. *J. Am. Ceram. Soc.* **1991**, *74*, 1487–1510. [CrossRef]

196. Hsieh, J.H.; Yeh, T.H.; Hung, S.Y.; Chang, S.Y.; Wu, W.; Li, C. Antibacterial and tribological properties of TaN–Cu, TaN–Ag, and TaN–(Ag,Cu) nanocomposite thin films. *Mater. Res. Bull.* **2012**, *47*, 2999–3003. [CrossRef]

197. van Hengel, I.A.J.; Tierolf, M.; Valerio, V.P.M.; Minneboo, M.; Fluit, A.C.; Fratila-Apachitei, L.E.; Apachitei, I.; Zadpoor, A.A. Self-defending additively manufactured bone implants bearing silver and copper nanoparticles. *J. Mater. Chem. B* **2020**, *8*, 1589–1602. [CrossRef] [PubMed]

198. Qin, H.; Cao, H.; Zhao, Y.; Jin, G.; Cheng, M.; Wang, J.; Jiang, Y.; An, Z.; Zhang, X.; Liu, X. Antimicrobial and osteogenic properties of silver-ion-implanted stainless steel. *ACS Appl. Mater. Interfaces* **2015**, *7*, 10785–10794. [CrossRef] [PubMed]

199. Qin, H.; Zhao, Y.; An, Z.; Cheng, M.; Wang, Q.; Cheng, T.; Wang, Q.; Wang, J.; Jiang, Y.; Zhang, X. Enhanced antibacterial properties, biocompatibility, and corrosion resistance of degradable Mg-Nd-Zn-Zr alloy. *Biomaterials* **2015**, *53*, 211–220. [CrossRef] [PubMed]

200. Chen, J.; Zhang, Y.; Ibrahim, M.; Etim, I.P.; Tan, L.; Yang, K. In vitro degradation and antibacterial property of a copper-containing micro-arc oxidation coating on Mg-2Zn-1Gd-0.5 Zr alloy. *Colloids Surf. B Biointerfaces* **2019**, *179*, 77–86. [CrossRef]

201. Qing, Y.; Cheng, L.; Li, R.; Liu, G.; Zhang, Y.; Tang, X.; Wang, J.; Liu, H.; Qin, Y. Potential antibacterial mechanism of silver nanoparticles and the optimization of orthopedic implants by advanced modification technologies. *Int. J. Nanomed.* **2018**, *13*, 3311–3327. [CrossRef]

202. Liu, X.; Gan, K.; Liu, H.; Song, X.; Chen, T.; Liu, C. Antibacterial properties of nano-silver coated PEEK prepared through magnetron sputtering. *Dent. Mater.* **2017**, *33*, e348–e360. [CrossRef]

203. Uhm, S.H.; Song, D.H.; Kwon, J.S.; Lee, S.B.; Han, J.G.; Kim, K.N. Tailoring of antibacterial Ag nanostructures on TiO2 nanotube layers by magnetron sputtering. *J. Biomed. Mater. Res. B Appl. Biomater.* **2014**, *102*, 592–603. [CrossRef] [PubMed]

204. Jia, Z.; Xiu, P.; Li, M.; Xu, X.; Shi, Y.; Cheng, Y.; Wei, S.; Zheng, Y.; Xi, T.; Cai, H. Bioinspired anchoring AgNPs onto micro-nanoporous TiO2 orthopedic coatings: Trap-killing of bacteria, surface-regulated osteoblast functions and host responses. *Biomaterials* **2016**, *100*, 203–222. [CrossRef] [PubMed]

205. Chen, Y.; Deng, Y.; Pu, Y.; Tang, B.; Su, Y.; Tang, J. One pot preparation of silver nanoparticles decorated TiO2 mesoporous microspheres with enhanced antibacterial activity. *Mater. Sci. Eng. C* **2016**, *100*, 27–32. [CrossRef]

206. Kamaraj, K.; George, R.; Anandkumar, B.; Parvathavarthini, N.; Kamachi, U.M. A silver nanoparticle loaded TiO2 nanoporous layer for visible light induced antimicrobial applications. *Bioelectrochemistry* **2015**, *106*, 290–297. [CrossRef] [PubMed]

207. Xu, Z.; Li, M.; Li, X.; Liu, X.; Ma, F.; Wu, S.; Yeung, K.W.; Han, Y.; Chu, P.K. Antibacterial Activity of Silver Doped Titanate Nanowires on Ti Implants. *ACS Appl. Mater. Interfaces* **2016**, *8*, 16584–16594. [CrossRef]

208. Lu, T.; Qiao, Y.; Liu, X. Surface modification of biomaterials using plasma immersion ion implantation and deposition. *Interface Focus* **2012**, *2*, 325–336. [CrossRef] [PubMed]

209. Cao, H.; Zhang, W.; Meng, F.; Guo, J.; Wang, D.; Qian, S.; Jiang, X.; Liu, X.; Chu, P.K. Osteogenesis Catalyzed by Titanium-Supported Silver Nanoparticles. *ACS Appl. Mater. Interfaces* **2017**, *9*, 5149–5157. [CrossRef] [PubMed]

210. Lai, H.; Qiao, S.; Cao, H.; Zhao, X.; Lo, H.; Zhuang, L.; Gu, Y.; Shi, J.; Liu, X. Ag-plasma modification enhances bone apposition around titanium dental implants: An animal study in Labrador dogs. *Int. J. Nanomed.* **2015**, *10*, 653–664. [CrossRef] [PubMed]

211. Lu, X.; Mohedano, M.; Blawert, C.; Matykina, E.; Arrabal, R.; Kainer, K.U.; Zheludkevich, M.L. Plasma electrolytic oxidation coatings with particle additions—A review. *Surf. Coat. Technol.* **2016**, *307*, 1165–1182. [CrossRef]

212. Necula, B.S.; Fratila-Apachitei, L.E.; Zaat, S.A.; Apachitei, I.; Duszczyk, J. In vitro antibacterial activity of porous TiO2–Ag composite layers against methicillin-resistant Staphylococcus aureus. *Acta Biomater.* **2009**, *5*, 3573–3580. [CrossRef]

213. Zhang, X.; Li, J.; Wang, X.; Wang, Y.; Hang, R.; Huang, X.; Tang, B.; Chu, P.K. Effects of copper nanoparticles in porous TiO2 coatings on bacterial resistance and cytocompatibility of osteoblasts and endothelial cells. *Mater. Sci. Eng. C* **2018**, *82*, 110–120. [CrossRef] [PubMed]

214. Dong, Y.; Ye, H.; Liu, Y.; Xu, L.; Wu, Z.; Hu, X.; Ma, J.; Pathak, J.L.; Liu, J.; Wu, G. pH dependent silver nanoparticles releasing titanium implant: A novel therapeutic approach to control peri-implant infection. *Colloids Surf. B Biointerfaces* **2017**, *158*, 127–136. [CrossRef] [PubMed]

215. Pang, X.; Zhitomirsky, I. Electrodeposition of hydroxyapatite–silver–chitosan nanocomposite coatings. *Surf. Coat. Technol.* **2008**, *202*, 3815–3821. [CrossRef]

216. Zhao, Y.; Cao, H.; Qin, H.; Cheng, T.; Qian, S.; Cheng, M.; Peng, X.; Wang, J.; Zhang, Y.; Jin, G. Balancing the osteogenic and antibacterial properties of titanium by codoping of Mg and Ag: An in vitro and in vivo study. *ACS Appl. Mater. Interfaces* **2015**, *7*, 17826–17836. [CrossRef]

217. Hsieh, J.; Tseng, C.; Chang, Y.; Chang, S.; Wu, W. Antibacterial behavior of TaN–Ag nanocomposite thin films with and without annealing. *Surf. Coat. Technol.* **2008**, *202*, 5586–5589. [CrossRef]

218. Huang, H.-L.; Chang, Y.-Y.; Chen, H.-J.; Chou, Y.-K.; Lai, C.-H.; Chen, M.Y. Antibacterial properties and cytocompatibility of tantalum oxide coatings with different silver content. *J. Vac. Sci. Technol. A Vac. Surf. Film.* **2014**, *32*, 02B117. [CrossRef]

219. Mejía, H.; Echavarría, A.M.; Bejarano, G. Influence of Ag-Cu nanoparticles on the microstructural and bactericidal properties of TiAlN (Ag, Cu) coatings for medical applications deposited by Direct Current (DC) magnetron sputtering. *Thin Solid Film.* **2019**, *687*, 137460. [CrossRef]

220. Rtimi, S.; Sanjines, R.; Pulgarin, C.; Kiwi, J. Quasi-instantaneous bacterial inactivation on Cu–ag nanoparticulate 3D catheters in the dark and under light: Mechanism and dynamics. *ACS Appl. Mater. Interfaces* **2016**, *8*, 47–55. [CrossRef]

221. Kedziora, A.; Korzekwa, K.; Strek, W.; Pawlak, A.; Doroszkiewicz, W.; Bugla-Ploskonska, G. Silver nanoforms as a therapeutic agent for killing Escherichia coli and certain ESKAPE pathogens. *Curr. Microbiol.* **2016**, *73*, 139–147. [CrossRef]

222. Zhong, X.; Song, Y.; Yang, P.; Wang, Y.; Jiang, S.; Zhang, X.; Li, C. Titanium surface priming with phase-transited lysozyme to establish a silver nanoparticle-loaded chitosan/hyaluronic acid antibacterial multilayer via layer-by-layer self-assembly. *PLoS ONE* **2016**, *11*, e0146957. [CrossRef] [PubMed]

223. Nazeruddin, G.; Prasad, R.; Shaikh, Y.; Shaikh, A. Synergetic effect of Ag-Cu bimetallic nanoparticles on antimicrobial activity. *Der. Pharm. Lett.* **2014**, *3*, 129–136.

224. Kushwah, M.; Gaur, M.; Berlina, A.N.; Arora, K. Biosynthesis of novel Ag@ Cu alloy NPs for enhancement of methylene blue photocatalytic activity and antibacterial activity. *MRE* **2019**, *6*, 116561. [CrossRef]

225. Rajendaran, K.; Muthuramalingam, R.; Ayyadurai, S. Green synthesis of Ag-Mo/CuO nanoparticles using Azadirachta indica leaf extracts to study its solar photocatalytic and antimicrobial activities. *Mater. Sci. Semicond. Process.* **2019**, *91*, 230–238. [CrossRef]

226. Tsuji, M.; Hikino, S.; Tanabe, R.; Matsunaga, M.; Sano, Y. Syntheses of Ag/Cu alloy and Ag/Cu alloy core Cu shell nanoparticles using a polyol method. *CrystEngComm* **2010**, *12*, 3900–3908. [CrossRef]

227. Dou, Q.; Yang, L.; Wong, K.W.; Ng, K.M. Facile synthesis of nearly monodisperse AgCu alloy nanoparticles with synergistic effect against oxidation and electromigration. *J. Mater. Res.* **2019**, *34*, 2095–2104. [CrossRef]

228. Zhao, J.; Zhang, D.; Zhao, J. Fabrication of Cu–Ag core–shell bimetallic superfine powders by eco-friendly reagents and structures characterization. *J. Solid State Chem.* **2011**, *184*, 2339–2344. [CrossRef]

229. Li, Y.-S.; Lu, Y.-C.; Chou, K.-S.; Liu, F.-J. Synthesis and characterization of silver–copper colloidal ink and its performance against electrical migration. *Mater. Res. Bull.* **2010**, *45*, 1837–1843. [CrossRef]

230. Vykoukal, V.; Halasta, V.; Babiak, M.; Bursik, J.; Pinkas, J. Morphology Control in AgCu Nanoalloy Synthesis by Molecular Cu(I) Precursors. *Inorg. Chem.* **2019**, *58*, 15246–15254. [CrossRef] [PubMed]

231. Syed, F.S.; Kasabe, A.M.; Mane, P.; Chaudhari, R.; Adhyapak, P. Selective antifungal and antibacterial activities of Ag-Cu and Cu-Ag core-shell nanostructures synthesized in-situ PVA. *Nanotechnology* **2020**. [CrossRef]

232. Liu, X.; Du, J.; Shao, Y.; Zhao, S.F.; Yao, K.F. One-pot preparation of nanoporous Ag-Cu@Ag core-shell alloy with enhanced oxidative stability and robust antibacterial activity. *Sci. Rep.* **2017**, *7*, 10249. [CrossRef] [PubMed]

233. Wang, X.; Li, R.; Li, Z.; Xiao, R.; Chen, X.-B.; Zhang, T. Design and preparation of nanoporous Ag–Cu alloys by dealloying Mg–(Ag,Cu)–Y metallic glasses for antibacterial applications. *J. Mater. Chem. B* **2019**, *7*, 4169–4176. [CrossRef]

234. Li, R.; Wu, N.; Liu, J.; Jin, Y.; Chen, X.-B.; Zhang, T. Formation and evolution of nanoporous bimetallic Ag-Cu alloy by electrochemically dealloying Mg-(Ag-Cu)-Y metallic glass. *Corros. Sci.* **2017**, *100*, 23–32. [CrossRef]

235. Satya Bharati, M.S.; Chandu, B.; Rao, S.V. Explosives sensing using Ag–Cu alloy nanoparticles synthesized by femtosecond laser ablation and irradiation. *RSC Adv.* **2019**, *9*, 1517–1525. [CrossRef]

236. Malviya, K.D.; Chattopadhyay, K. High quality oxide-free metallic nanoparticles: A strategy for synthesis through laser ablation in aqueous medium. *J. Mater. Sci.* **2014**, *50*, 980–989. [CrossRef]

237. Malviya, K.D.; Chattopadhyay, K. Synthesis and mechanism of composition and size dependent morphology selection in nanoparticles of Ag–Cu alloys processed by laser ablation under liquid medium. *J. Phys. Chem. C* **2014**, *118*, 13228–13237. [CrossRef]

238. Muzikansky, A.; Nanikashvili, P.; Grinblat, J.; Zitoun, D. Ag dewetting in Cu@ Ag monodisperse core–shell nanoparticles. *J. Phys. Chem. C* **2013**, *117*, 3093–3100. [CrossRef]

239. Kim, N.R.; Shin, K.; Jung, I.; Shim, M.; Lee, H.M. Ag–Cu bimetallic nanoparticles with enhanced resistance to oxidation: A combined experimental and theoretical study. *J. Phys. Chem. C* **2014**, *118*, 26324–26331. [CrossRef]

240. Lee, C.; Kim, N.R.; Koo, J.; Lee, Y.J.; Lee, H.M. Cu-Ag core–shell nanoparticles with enhanced oxidation stability for printed electronics. *Nanotechnology* **2015**, *26*, 455601. [CrossRef]

241. Chen, X.; Ku, S.; Weibel, J.A.; Ximenes, E.; Liu, X.; Ladisch, M.; Garimella, S.V. Enhanced antimicrobial efficacy of bimetallic porous CuO microspheres decorated with Ag nanoparticles. *ACS Appl. Mater. Interfaces* **2017**, *9*, 39165–39173. [CrossRef] [PubMed]

242. Ma, J.; Guo, S.; Guo, X.; Ge, H. Preparation, characterization and antibacterial activity of core–shell Cu2O@ Ag composites. *Surf. Coat. Technol.* **2015**, *100*, 268–272. [CrossRef]

243. Yao, Y.; Huang, Z.; Xie, P.; Lacey, S.D.; Jacob, R.J.; Xie, H.; Chen, F.; Nie, A.; Pu, T.; Rehwoldt, M. Carbothermal shock synthesis of high-entropy-alloy nanoparticles. *Science* **2018**, *359*, 1489–1494. [CrossRef] [PubMed]

244. Ceylan, A.; Jastrzembski, K.; Shah, S.I. Enhanced solubility Ag-Cu nanoparticles and their thermal transport properties. *Metall. Mater. Trans. A* **2006**, *37*, 2033–2038. [CrossRef]

245. Bakina, O.; Glazkova, E.; Pervikov, A.; Lozhkomoev, A.; Rodkevich, N.; Svarovskaya, N.; Lerner, M.; Naumova, L.; Varnakova, E.; Chjou, V. Design and Preparation of Silver–Copper Nanoalloys for Antibacterial Applications. *J. Clust. Sci.* **2020**, *31*, 1–8. [CrossRef]
246. Rousse, C.; Josse, J.; Mancier, V.; Levi, S.; Gangloff, S.C.; Fricoteaux, P. Synthesis of copper–silver bimetallic nanopowders for a biomedical approach; study of their antibacterial properties. *RSC Adv.* **2016**, *6*, 50933–50940. [CrossRef]
247. Mancier, V.; Rousse-Bertrand, C.; Dille, J.; Michel, J.; Fricoteaux, P. Sono and electrochemical synthesis and characterization of copper core–Silver shell nanoparticles. *Ultrason. Sonochem.* **2010**, *17*, 690–696. [CrossRef]
248. Tchaplyguine, M.; Andersson, T.; Zhang, C.; Björneholm, O. Core-shell structure disclosed in self-assembled Cu-Ag nanoalloy particles. *J. Chem. Phys.* **2013**, *138*, 104303. [CrossRef] [PubMed]
249. Ferrando, R.; Jellinek, J.; Johnston, R.L. Nanoalloys: From theory to applications of alloy clusters and nanoparticles. *Chem. Rev.* **2008**, *108*, 845–910. [CrossRef]
250. Srinoi, P.; Chen, Y.-T.; Vittur, V.; Marquez, M.D.; Lee, T.R. Bimetallic nanoparticles: Enhanced magnetic and optical properties for emerging biological applications. *Appl. Sci.* **2018**, *8*, 1106. [CrossRef]
251. Scott, D.A. *Metallography and Microstructure in Ancient and Historic Metals*; Averkieff, I., Ed.; Getty Publications: Singapore, 1992.
252. Koo, W.-T.; Millstone, J.E.; Weiss, P.S.; Kim, I.-D. The Design and Science of Polyelemental Nanoparticles. *ACS Nano* **2020**, *14*, 6407–6413. [CrossRef]
253. Chen, P.-C.; Liu, X.; Hedrick, J.L.; Xie, Z.; Wang, S.; Lin, Q.-Y.; Hersam, M.C.; Dravid, V.P.; Mirkin, C.A. Polyelemental nanoparticle libraries. *Science* **2016**, *352*, 1565–1569. [CrossRef]
254. Malviya, K.D.; Chattopadhyay, K. Temperature- and Size-Dependent Compositionally Tuned Microstructural Landscape for Ag-46 Atom % Cu Nanoalloy Prepared by Laser Ablation in Liquid. *J. Phys. Chem. C* **2016**, *120*, 27699–27706. [CrossRef]
255. Marks, R.A.; Glaeser, A.M. Effects of phase fraction on phase morphology and triple junction configuration in anisotropic systems. *Acta Mater.* **2012**, *60*, 4563–4574. [CrossRef]
256. Li, A.; Szlufarska, I. Morphology and mechanical properties of nanocrystalline Cu/Ag alloy. *J. Mater. Sci.* **2017**, *52*, 4555–4567. [CrossRef]
257. Ke, X.; Ye, J.; Pan, Z.; Geng, J.; Besser, M.F.; Qu, D.; Caro, A.; Marian, J.; Ott, R.T.; Wang, Y.M.; et al. Ideal maximum strengths and defect-induced softening in nanocrystalline-nanotwinned metals. *Nat. Mater.* **2019**, *18*, 1207–1214. [CrossRef] [PubMed]
258. Hua, X.; Li, H.W.; Long, Y.T. Investigation of Silver Nanoparticle Induced Lipids Changes on a Single Cell Surface by Time-of-Flight Secondary Ion Mass Spectrometry. *Anal. Chem.* **2018**, *90*, 1072–1076. [CrossRef]
259. Kim, Y.P.; Shon, H.K.; Shin, S.K.; Lee, T.G. Probing nanoparticles and nanoparticle-conjugated biomolecules using time-of-flight secondary ion mass spectrometry. *Mass Spectrom. Rev.* **2015**, *34*, 237–247. [CrossRef]
260. Wu, C.-K.; Yin, M.; O'Brien, S.; Koberstein, J.T. Quantitative analysis of copper oxide nanoparticle composition and structure by X-ray photoelectron spectroscopy. *Chem. Mater.* **2006**, *18*, 6054–6058. [CrossRef]
261. Jiménez, J.A.; Liu, H.; Fachini, E. X-ray photoelectron spectroscopy of silver nanoparticles in phosphate glass. *Mater. Lett.* **2010**, *64*, 2046–2048. [CrossRef]
262. Mallick, S.; Sanpui, P.; Ghosh, S.S.; Chattopadhyay, A.; Paul, A. Synthesis, characterization and enhanced bactericidal action of a chitosan supported core–shell copper–silver nanoparticle composite. *RSC Adv.* **2015**, *5*, 12268–12276. [CrossRef]
263. Veith, L.; Dietrich, D.; Vennemann, A.; Breitenstein, D.; Engelhard, C.; Karst, U.; Sperling, M.; Wiemann, M.; Hagenhoff, B. Combination of micro X-ray fluorescence spectroscopy and time-of-flight secondary ion mass spectrometry imaging for the marker-free detection of CeO2 nanoparticles in tissue sections. *J. Anal. At. Spectrom.* **2018**, *33*, 491–501. [CrossRef]
264. Nowak, A.; Szade, J.; Talik, E.; Zubko, M.; Wasilkowski, D.; Dulski, M.; Balin, K.; Mrozik, A.; Peszke, J. Physicochemical and antibacterial characterization of ionocity Ag/Cu powder nanoparticles. *Mater. Charact.* **2016**, *100*, 9–16. [CrossRef]
265. Wang, Z. Transmission electron microscopy of shape-controlled nanocrystals and their assemblies. *J. Phys. Chem. B* **2000**, *104*, 1153–1175. [CrossRef]
266. Sondi, I.; Salopek-Sondi, B. Silver nanoparticles as antimicrobial agent: A case study on E. coli as a model for Gram-negative bacteria. *J. Colloid Interface Sci.* **2004**, *275*, 177–182. [CrossRef] [PubMed]
267. Biswas, P.; Bandyopadhyaya, R. Synergistic antibacterial activity of a combination of silver and copper nanoparticle impregnated activated carbon for water disinfection. *Environ. Sci. Nano* **2017**, *4*, 2405–2417. [CrossRef]
268. Yu, X.; Li, J.; Shi, T.; Cheng, C.; Liao, G.; Fan, J.; Li, T.; Tang, Z. A green approach of synthesizing of Cu-Ag core-shell nanoparticles and their sintering behavior for printed electronics. *J. Alloys Compd.* **2017**, *724*, 365–372. [CrossRef]
269. Shindo, D.; Oikawa, T. Energy dispersive x-ray spectroscopy. In *Analytical Electron Microscopy for Materials Science*; Shindo, D., Oikawa, T., Eds.; Springer: Tokyo, Japan, 2002; pp. 81–102.
270. Kril, C.; Birringer, R. Estimating grain-size distributions in nanocrystalline materials from X-ray diffraction profile analysis. *Philos. Mag. A* **1998**, *77*, 621–640. [CrossRef]
271. Yang, Z.; Ma, C.; Wang, W.; Zhang, M.; Hao, X.; Chen, S. Fabrication of Cu2O-Ag nanocomposites with enhanced durability and bactericidal activity. *J. Colloid Interface Sci.* **2019**, *557*, 156–167. [CrossRef] [PubMed]
272. Zhou, M.; Wang, Z.; Sun, Q.; Wang, J.; Zhang, C.; Chen, D.; Li, X. High-performance Ag–Cu nanoalloy catalyst for the selective catalytic oxidation of ammonia. *ACS Appl. Mater. Interfaces* **2019**, *11*, 46875–46885. [CrossRef]
273. Prater, C.; Kjoller, K.; Shetty, R. Nanoscale infrared spectroscopy. *Mater. Today* **2010**, *13*, 56–60. [CrossRef]

274. Dazzi, A.; Prater, C.B.; Hu, Q.; Chase, D.B.; Rabolt, J.F.; Marcott, C. AFM–IR: Combining atomic force microscopy and infrared spectroscopy for nanoscale chemical characterization. *Appl. Spectrosc.* **2012**, *66*, 1365–1384. [CrossRef]
275. Zia, R.; Riaz, M.; Farooq, N.; Qamar, A.; Anjum, S. Antibacterial activity of Ag and Cu nanoparticles synthesized by chemical reduction method: A comparative analysis. *MRE* **2018**, *5*, 075012. [CrossRef]
276. Cui, L.; Chen, P.; Chen, S.; Yuan, Z.; Yu, C.; Ren, B.; Zhang, K. In situ study of the antibacterial activity and mechanism of action of silver nanoparticles by surface-enhanced Raman spectroscopy. *Anal. Chem.* **2013**, *85*, 5436–5443. [CrossRef]
277. Guzman, M.; Dille, J.; Godet, S. Synthesis and antibacterial activity of silver nanoparticles against gram-positive and gram-negative bacteria. *Nanomedicine* **2012**, *8*, 37–45. [CrossRef]
278. Hans, M.; Támara, J.C.; Mathews, S.; Bax, B.; Hegetschweiler, A.; Kautenburger, R.; Solioz, M.; Mücklich, F. Laser cladding of stainless steel with a copper–silver alloy to generate surfaces of high antimicrobial activity. *Appl. Surf. Sci.* **2014**, *100*, 195–199. [CrossRef]
279. Hong, H.R.; Kim, J.; Park, C.H. Facile fabrication of multifunctional fabrics: Use of copper and silver nanoparticles for antibacterial, superhydrophobic, conductive fabrics. *RSC Adv.* **2018**, *8*, 41782–41794. [CrossRef]
280. Yang, L.; Chen, L.; Chen, Y.C.; Kang, L.; Yu, J.; Wang, Y.; Lu, C.; Mashimo, T.; Yoshiasa, A.; Lin, C.H. Homogeneously alloyed nanoparticles of immiscible Ag-Cu with ultrahigh antibacterial activity. *Colloids Surf. B Biointerfaces* **2019**, *180*, 466–472. [CrossRef]
281. Elsayed, D.; Abdelbasir, S.; Abdel-Ghafar, H.; Salah, B.; Sayed, S. Silver and copper nanostructured particles recovered from metalized plastic waste for antibacterial applications. *J. Environ. Chem. Eng.* **2020**, *8*, 103826. [CrossRef]
282. Joshi, B.; Regmi, C.; Dhakal, D.; Gyawali, G.; Lee, S.W. Efficient inactivation of Staphylococcus aureus by silver and copper loaded photocatalytic titanate nanotubes. *Prog. Nat. Sci. Mater. Int.* **2018**, *28*, 15–23. [CrossRef]
283. Khare, P.; Sharma, A.; Verma, N. Synthesis of phenolic precursor-based porous carbon beads in situ dispersed with copper–silver bimetal nanoparticles for antibacterial applications. *J. Colloid Interface Sci.* **2014**, *418*, 216–224. [CrossRef] [PubMed]
284. Perdikaki, A.; Galeou, A.; Pilatos, G.; Karatasios, I.; Kanellopoulos, N.K.; Prombona, A.; Karanikolos, G.N. Ag and Cu monometallic and Ag/Cu bimetallic nanoparticle–graphene composites with enhanced antibacterial performance. *ACS Appl. Mater. Interfaces* **2016**, *8*, 27498–27510. [CrossRef]
285. Ali, A.; Baheti, V.; Vik, M.; Militky, J. Copper electroless plating of cotton fabrics after surface activation with deposition of silver and copper nanoparticles. *J. Phys. Chem. Solids* **2020**, *137*. [CrossRef]
286. Mohsen, R.; Mohamed, S.; Abu-ayana, Y.; Ghoneim, A. Synthesis of Conductive Cu-core/Ag-subshell/polyaniline-shell Nanocomposites and their Antimicrobial Activity. *Egypt. J. Chem.* **2018**, *61*, 939–952. [CrossRef]